Radiation

&EPA
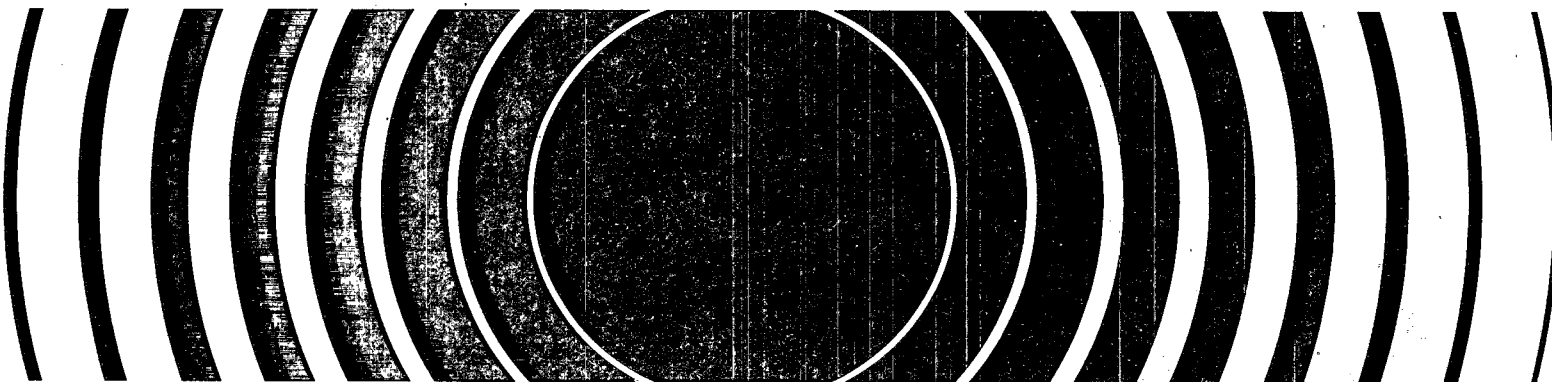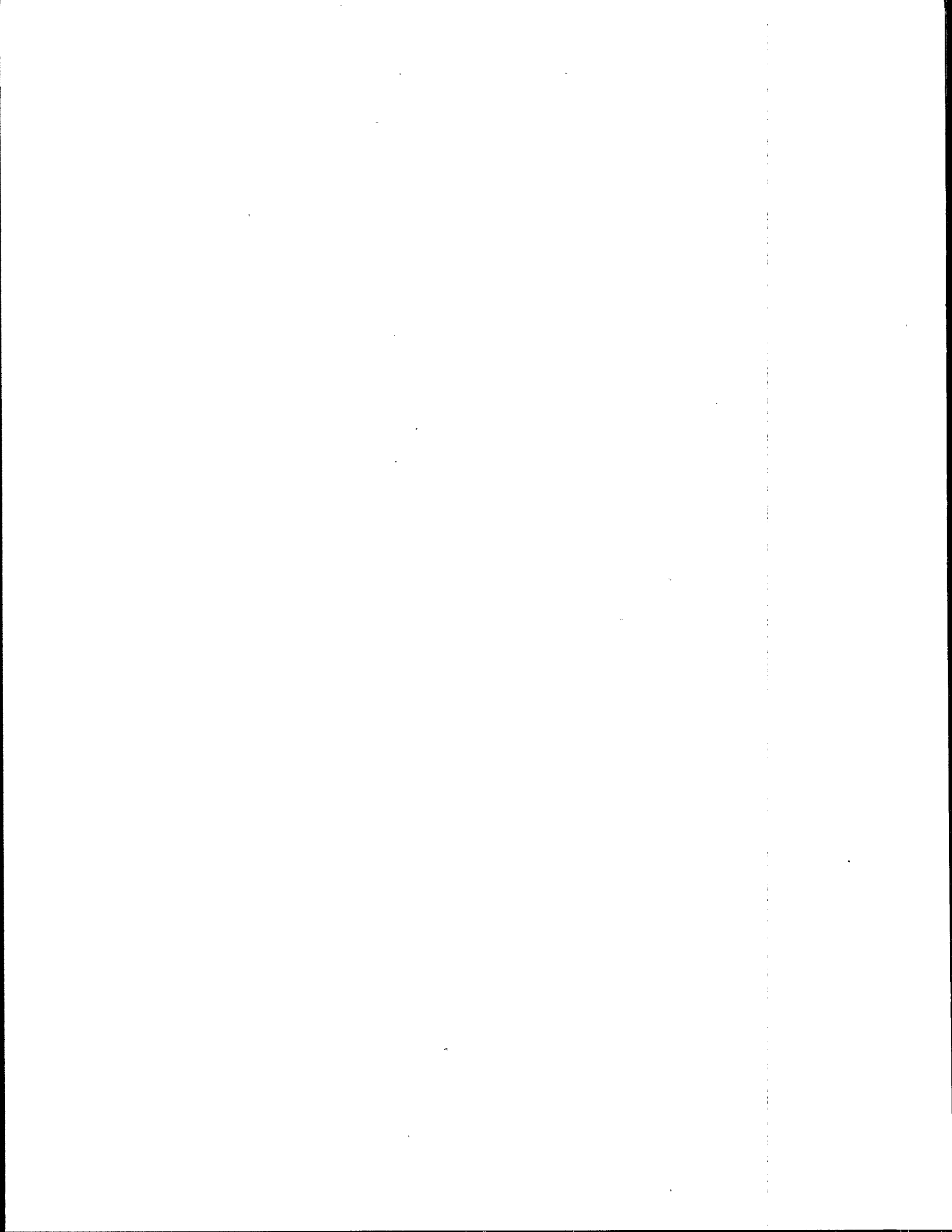
Prediction of Vertical Transport of Low-Level Radioactive Middlesex Soil at a Deep-Ocean Disposal Site

PREDICTION OF VERTICAL TRANSPORT OF LOW-LEVEL RADIOACTIVE MIDDLESEX SOIL AT A DEEP-OCEAN DISPOSAL SITE

by

James S. Bonner
Applied Technology Division
Computer Sciences Corporation
EPA Environmental Research Laboratory
Narragansett, Rhode Island 02882

Carlton D. Hunt
Marine Ecosystems Research Laboratory
Graduate School of Oceanography
University of Rhode Island
Narragansett, Rhode Island 02882

John F. Paul and Victor J. Bierman, Jr.
Environmental Research Laboratory
Office of Environmental Processes and Effects Research
U.S. Environmental Protection Agency
South Ferry Road
Narragansett, Rhode Island 02882

DISCLAIMER

This report has been reviewed by the Environmental Research Laboratory, U.S. Environmental Protection Agency, Narragansett, Rhode Island, and approved for publication. Approval does not signify that the contents necesarily reflect the views and policies of the U.S. Environmental Protection Agency, nor does mention of trade-names or commercial products constitute endorsement or recommendation for use.
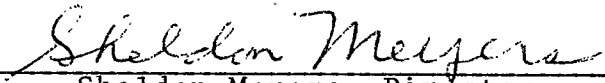
FOREWORD

In response to the mandate of Public Law 92-532, the Marine Protection, Research and Sanctuaries Act of 1972, as amended, the Environmental Protection Agency (EPA) has developed a program to promulgate regulations and criteria to control the ocean disposal of radioactive wastes. Interest expressed by other Government agencies has led EPA to consider the environmental fate of unpackaged soils, containing very low levels of naturally-occurring radioactivity, after surface disposal over a deep-sea site. An important technical factor in any environmental assessment of this disposal alternative for dry soils is the potential for physical transport of the material from the point of initial disposal at the ocean surface.

This report summarizes the data obtained through laboratory experiments using both small and large experimental tanks to simulate such a disposal operation. A model was then developed to predict deep-ocean transport. Model calculations were made to incorporate soil settling rates and physical and chemical properties which could influence the behavior of contaminants in the soil on initial contact with seawater and subsequent passage through the water column. The study was carried out in a manner consistent with the Hazard Assessment Strategy developed by the EPA Office of Water. The Hazard Assessment Strategy contains the scientific framework under which potential ocean disposal permit requests may be evaluated. The experimental methods, experimental results and modeling approach and application to predict deep-ocean transport are described, and conclusions drawn regarding fate of the soils if they were to be disposed of at the ocean surface over a 4,000 meter depth site.

The Office of Radiation Programs will use this report as an information base for any future inquiries regarding the ocean disposal of soils containing low levels of radio-activity. The methodologies described and the model developed may also be valuable for the environmental assessments of other kinds of pollutants proposed for ocean disposal in unpackaged form.

The Agency invites all readers of this report to send any comments or suggestions to Mr. David E. Janes, Director, Analysis and Support Division, Office of Radiation Programs (ANR-461), Environmental Protection Agency, Washington, D.C. 20460.

Sheldon Meyers, Director
Office of Radiation Programs (ANR-458)

ABSTRACT

Potential ocean disposal of low-level natural radioisotopes associated with soils was investigated by combining experimental and modeling approaches to determine transport and fate of the material. The work was accomplished within the framework of the hazard assessment methodology developed at the EPA Environmental Research Laboratory Narragansett. Source material was provided from a Department of Energy designated Formerly Utilized Sites Remedial Action Program (FUSRAP) site in Middlesex, New Jersey. The experimental approach involved characterization of the source material for particle size distribution, specific gravity, total radioisotope activity and distribution, nuclide soluble phase equilibria of the radioisotopes, and particle settling velocities.

Soil particles were primarily sandy with a size range from less than 63 microns to greater than 2000 microns and a specific gravity of 2.31. The median particle size for total gamma plus beta or total alpha counts (125 microns) was not coincident with the median grain size (350 microns). The individual radioisotopes Ra-226, U-234, U-238, and Th-230 exhibited similar distributions (median size of 250 microns), while the distributions for Pb-210 and Po-210 were shifted to the larger particle sizes. Radioisotopes were primarily associated with discrete soil particles and are assumed to be residuals of the original ores processed at the site. Less than 10 per cent of the associated radioisotopes leached from the soil after exposure to seawater for up to 20 hours. Particle settling velocities measured for a number of size classes in a 1 meter settling column ranged up to 8.2 cm/sec (median 2.1 cm/sec). Mesocosm-scale experiments confirmed that settling would be the dominant vertical transport mechanism for these soil particles at a deep-ocean disposal site.

The experimental results were used to calibrate a one-dimensional convective-diffusive particle transport model which was applied to a hypothetical ocean disposal site in 4000 m of water. The model predicted that 95 per cent of the soils and associated radioisotopes would impact the bottom sediments within 4.5 days. Addition of a horizontal transport component to the model indicated that 95 per cent of the soil mass would impact the bottom sediments within 40 km of the disposal point along the direction of mean flow, for typical currents observed off the northeast U.S. continental shelf.

An overall project with the FUSRAP material was conducted which involved physical-chemical (exposure) and ecosystem (fate/effects) components. The physical-chemical component is described in the work reported here. The ecosystem component is covered in a separate report.

This report covers a period from 1 January 1984 to 30 April 1985, and work was completed as of 30 April 1985.

CONTENTS

v

FIGURES

TABLES

ACKNOWLEDGEMENTS

SECTION 1

INTRODUCTION

BACKGROUND

The Marine Protection, Research and Sanctuaries Act of 1972 (33 U. S. C. 1401), commonly referred to as the Ocean Dumping Act, authorizes the Environmental Protection Agency (EPA) to regulate all ocean disposal activities in the United States, including disposal of radioactive wastes not specifically prohibited by law. Under the provisions of this Act, EPA is also required to establish and apply criteria for review and evaluation of disposal permit applications. In 1981 Sandia National Laboratories initiated an evaluation of potential disposal sites, including the oceans, for soils contaminated with low, but significant, levels of natural radioisotopes under the Department of Energy's Formerly Utilized Sites Remedial Action Program (FUSRAP). This program was designed to evaluate and clean up numerous inactive industrial plant sites remaining from the Manhattan Project (Kupferman et al., 1984). Sandia identified the sampling plant material at Middlesex, New Jersey, as a candidate for potential ocean disposal. Efforts were begun to document the feasibility and advantages of ocean disposal of the soils and rubble from this site and to support potential permit applications to EPA (Kupferman et al., 1984).

In order to assist the EPA Office of Radiation Programs in evaluating potential permit applications of this type, the EPA Environmental Research Laboratory – Narragansett (ERLN) proposed that a hazard or risk assessment methodology (Prager et al., 1984) be developed specific to disposal of low-level radioactive waste in the oceans. The principal objective of this effort was to develop a useful, scientifically credible framework within which the potential permitting process could be undertaken. This methodology required several distinct types of effort including waste characterization, site selection, and determination of exposure fields and potential biological impacts at any of several levels of sophistication (Figure 1).

Preliminary characterization of the site in Middlesex by Sandia had identified several potential contaminants including natural radionuclides and inorganic and organic toxins (Kupferman et al., 1984). Of these, only radioisotopes were at levels to be of potential concern. In addition, Sandia identified the 106-Mile Ocean Disposal Site, a previously designated site for industrial waste disposal in the northwest Atlantic off of the continental shelf, as a candidate site to receive the soils (Kupferman et al., 1984).

SCOPE

The Sandia studies and results were useful but not sufficient to develop and test the hazard assessment methodology. This methodology
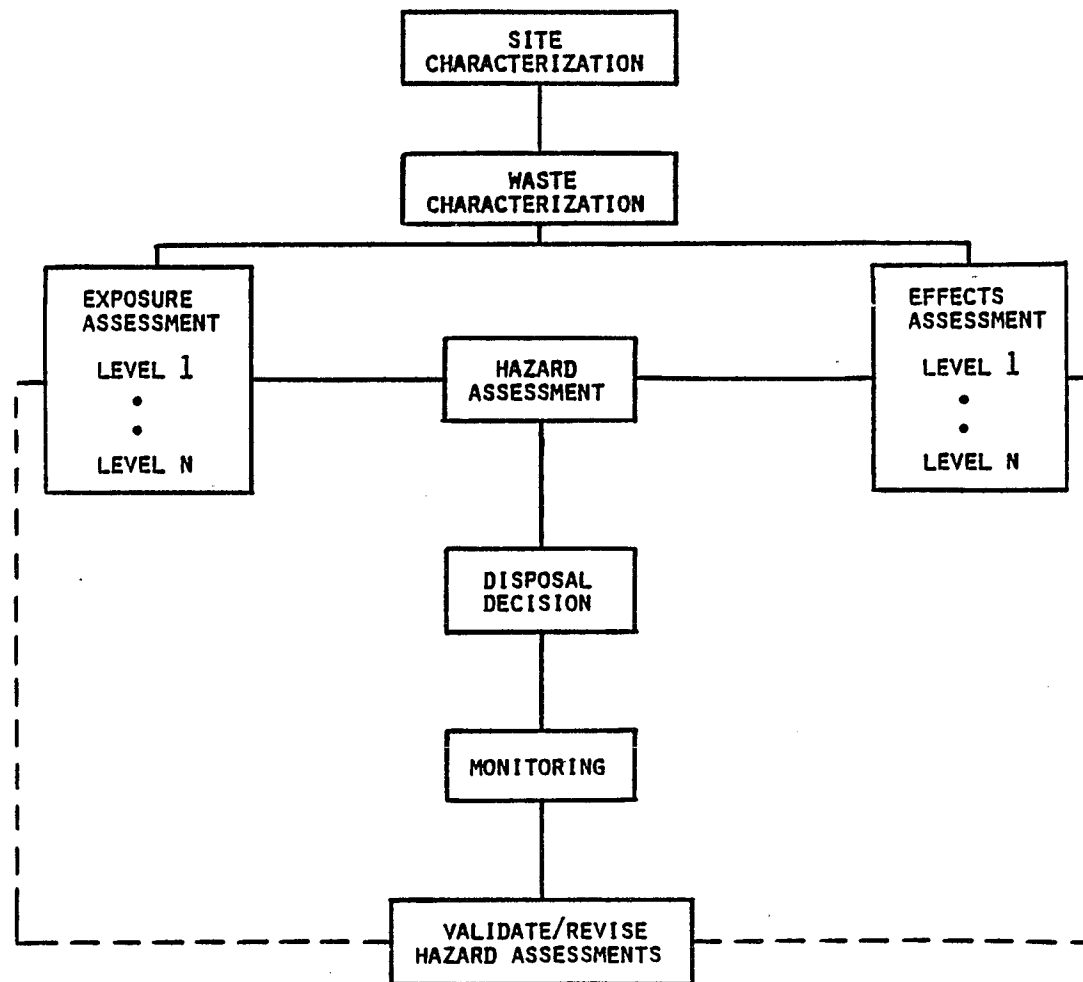
Figure 1. Hazard assessment strategy for ocean disposal.

specificially required better understanding of the exposure fields
which would result from disposal of this soil in the marine
environment. Since field measurements are difficult to obtain without
an actual disposal operation, it was determined that a
laboratory-scale experimental effort be combined with a modeling
approach to provide the necessary transport information. The
availability of soils from a designated FUSRAP, now FODOCS
(Feasibility of Disposal of Contaminated Soils), site allowed us to
conduct experiments with a specific low-level radioactive material,
within the context of the hazard assessment methodology.

Development of the model required estimates of soil settling
rates and physical and chemical properties that would modify the
contaminants in the soil on contact and passage through sea water.
Specifically, it was necessary to:

1. Characterize the Middlesex soil for parameters affecting
    transport.

2. Develop and calibrate a vertical transport model using data
    from 1.

3. Apply this model to estimate the transport and fate of the
    radioisotopes at a hypothetical deep-ocean disposal site.

The experimental efforts necessary for this development included:

1. Measurement of particle specific gravity, size and activity
    distributions, and radionuclide dissolution for
    representative soils from the Middlesex site.

2. Construction of a laboratory bench scale settling column and
    measurement of dynamic soil settling velocity distributions
    under quiescent hydrodynamic conditions.

3. Simulation of deep-ocean vertical dispersion conditions and
    quantification of vertical dispersion over a range of ocean
    values by modification of large scale water columns
    (mesocosms) at the Marine Ecosystems Research Laboratory
    (MERL), University of Rhode Island.

4. Measurement of vertical transport of Middlesex soil in the
    mesocosms under vertical dispersion conditions typical of the
    deep ocean.

The model used to describe transport of this soil in the ocean
depended on the characteristics of the soil and behavior of associated
contaminants. Tightly bound contaminants required a description of
particle transport alone to determine the contaminant exposure
concentration fields. If, however, a significant fraction of the
contaminant had not remained associated with the particulate matrix,

then the modeling approach would also have had to consider a soluble contaminant phase. In either case, radioisotope distributions for the source material were required to predict transport and fate, particularly if the activity was unevenly distributed throughout the particle size spectrum. In this case, model development would have focused on the transport of specific particle size classes which had the significant levels of radioactivity.

Our efforts demonstrated that a particulate convective-diffusive model was sufficient to describe the transport and fate of natural radionuclides associated with soil from the FUSRAP site. This model predicted that the vast majority of soils would impact the bottom sediments at a 4000 m disposal site within 4.5 days and up to 40 km away, along the direction of mean flow for typical currents observed off the northeast U.S. continental shelf.

SECTION 2

EXPERIMENTAL METHODS

SOIL SAMPLES

Representative samples of the soil from the Middlesex site were obtained in August 1982 by Sandia and MERL personnel. Samples of soil were excavated from the site, sieved through a 1/4 inch (ca. 6350 micron) mesh, characterized on site for total radioactivity, and combined into five separate 100 kg subsamples having different total radioactivity. Samples were homogenized at the site in a 0.15 m^3 standard cement mixer and divided into 50 kg replicate batches. These samples were distributed by Sandia for acute solid phase toxicity testing and an experiment involving the controlled marine ecosystem concept at MERL. One replicate of each sample was archived at Middlesex for possible future work. The results in this report are based on the sample sets (designated B1A and B) which had the highest activity (ca. 500 pCi Ra-226/g dry weight). Specific activity determinations were carried out in 1982 by Sandia and in 1984 by the Eastern Environmental Radiation Facilities (EERF) of EPA in Montgomery, Alabama. The activity in this sample is about 10 times higher than the mean for the total Middlesex site (Kupferman, personal communications).

SPECIFIC GRAVITY

Specific gravity of the Middlesex soil sample was determined using standard pycnometric procedures at 20 degrees centigrade. The average bulk specific gravity was 2.31. Throughout this study, this value was assumed for all size categories.

PARTICLE CHARACTERISTICS

Soil size distributions were measured by two methods. Method one involved quantitatively oven drying 100 g of soil at 70°C to determine percent moisture. The dried sample was then sieved for 20 minutes with a Ro-tap® particle sieve shaking system (Carver, 1971) using 0.5 Phi size increments between 4.0 and - 1.0 Phi units (63 to 2000 microns). The soil retained on each sieve was quantified in terms of mass and the mass percent, and a cumulative size distribution determined.

The second technique utilized a HIAC-SSTA automatic particle counter calibrated to count particles in 5 sizes between 20 and 600 microns. The counting sensor was positioned vertically at the bottom of a 1 m bench scale experimental settling column (discussed later), filled with 0.4 micron filtered lower Narragansett Bay sea water (salinity ca. 30 ppt). A known mass of soil was added at the top of the column and allowed to settle through it. Total particle counts were maintained at less than 100/ml to avoid coincidence counts with the sensor. The hydrostatic head from the column was sufficient to force the fluid through the sensor at 380 ml/min. Bias resulting from

differential particle arrival time was eliminated by continuing the experiment until background count rates were obtained. This method provided a measure of the dynamic behavior of the wetted particles. Particle counts were transformed to mass by multiplying average particle volume (assuming spherical particles) for a given size range by the measured average soil density. Comparison of size classes between the two techniques was accomplished by adjusting and normalizing the dry size results to correspond with the HIAC results.

ACTIVITY DISTRIBUTIONS

Particles obtained from the dry size classification procedure were analyzed for total radioactivity by two techniques. A gross measure of total activity was determined on each size class by counting total gamma plus beta and total alpha particles emanating from a known mass of sample with a Nuclear Measurements, Inc., PC-5 proportional counting system. Results were calculated in terms of disintegration per minute per gram dry sample (DPM/g) and corrected for incident background radiation. These same samples were then sent to EERF for quantification of radioisotopes Ra-226, Pb-210, Po-210, U-234, U-235, U-238, Th-227, Th-228, Th-230, and Th-232. In addition, autoradiography of the soil particles in several size classes showed the radioactivity in these samples was principally confined to discrete particles within the soil matrix and not homogeneously distributed on all particles.

SOLUBLE PHASE EQUILIBRIA

Dissolution of radioisotopes from the soil was examined with laboratory leaching methods and quantified by means of a partitioning coefficient, Kd, defined as:

$$KD = \frac{\text{mass of isotope/Kg solid}}{\text{mass of isotope/Kg sea water}} .$$

Four aliquots of the Middlesex soil sample B1A were suspended in a known volume of 0.4 micron filtered lower Narragansett Bay sea water. Samples were maintained at 20 degrees centigrade and intermittently mixed over 20 hours. Particulate and soluble fractions were then separated by filtration (0.45 micron) and each fraction analyzed for Ra-226, Pb-210, U-234, U-235, U-238, Th-227, Th-228, Th-230, and Th-232 at EERF.

SETTLING VELOCITY DISTRIBUTIONS

Soil settling velocities were determined with a laboratory bench scale settling column (Figure 2). The column was constructed from a 1 m long piece of 20 cm diameter PVC pipe. Transmissometers, interfaced to a microcomputer, were mounted externally on the side of the column (with glass windows) at depths of 16, 39, 62, and 85 cm to measure the attenuation of infrared light as a function of time caused by the
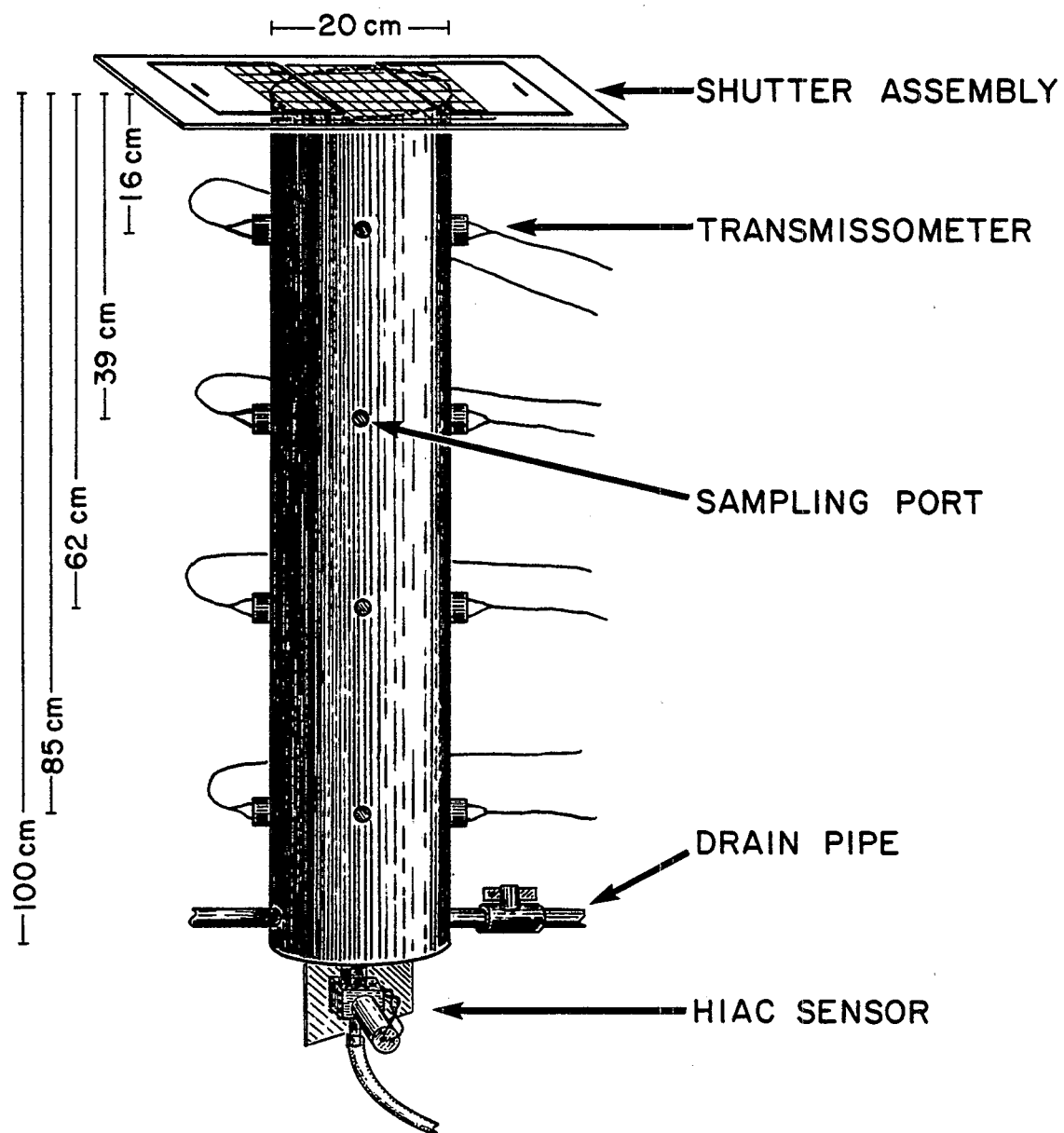
Figure 2. Laboratory settling column.

passage of particles.

A HIAC-SSTA electronic particle sensor was mounted vertically on the bottom plate of the column to determine the hydrated particle size distributions. Soil samples were added instantaneously across the entire surface area of the column by means of a gridded shutter, which was located 3 mm above the water surface. The shutter was interfaced with the microcomputer and triggered the transmissometer sampling when opening. Filtered (0.4 micron) lower Narragansett Bay seawater was added to the column before each experiment. The intensity of each transmissometer was matched by equalizing electronic outputs using filtered sea water in the column.

It was assumed that the light attenuation was proportional to the particle concentrations. This was tested by addition of four soil samples of known mass to the column. The integrated area of the transmissometer response versus time was found proportional to the mass of material added. It was also assumed that the ratio of attenuation to particle concentration was the same for all of the particle sizes.

As the particles settled past a transmissometer, the attentuation of the light beam increased as a direct function of the particle concentration. The analog signal was passed through an analog-to-digital converter, and the corresponding digital values were stored. The response, i.e., particle concentration, at each depth was integrated over time and normalized. A probability density function was calculated to provide estimates of the percent of the total mass passing a given depth as a function of time. The cumulative velocity distribution, for a given depth was calculated from the empirical relationship between cumulative sum of percent mass as a function of depth divided by time. The vertical velocity distribution was, therefore, determined by measuring the time of travel for each fraction of total mass through a known distance (velocity = distance/time). Probability and cumulative frequency curves were determined for each experimental run.

MESOCOSM-SCALE EXPERIMENTS

A series of experiments in MERL mesocosms were designed to quantify the effects of vertical dispersion on settling rates to provide more realistic mass transport estimates for the model predictions. These experiments were accomplished by modifying the normal up/down plunger mixing used by MERL (Nixon et al., 1980) with axially driven impellers which rotated 360 degrees in a clockwise/counterclockwise mode (Figure 3). This design provided uniform mixing throughout the water column, as quantified by dye studies.

The vertical dispersion in the mesocosm tanks was determined at three levels of mixing. This was accomplished by first allowing the impeller to operate at a set rate sufficiently long for a dynamic equilibrium to be established in the tank. Rhodamine-WT dye was then
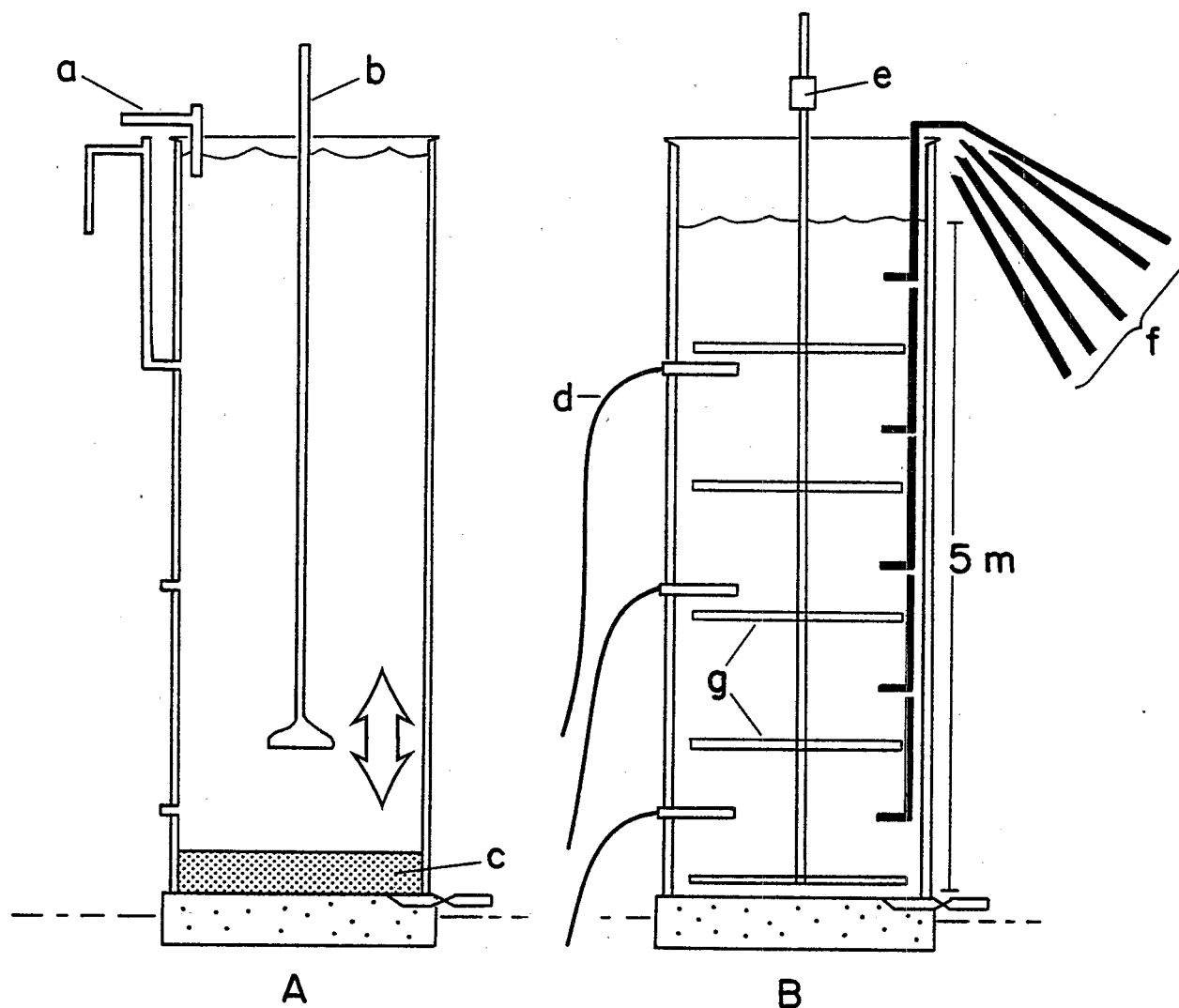
Figure 3. MERL mesocosm. A. Normal up/down plunger mixing. B. Axially driven impeller mixing. a. Inflow to mesocosm. b. Plunger. c. Sediments. d. Sampling ports for suspended solids measurements. e. Axially driven impeller. f. Sampling ports for dye measurements. g. Impeller.

sprayed onto the water surface and the concentration determined at 5 depths (0.5, 1.5, 2.5, 3.5, 4.5 m) as a function of time. Dye studies at mixing speeds of 0.37, 0.52, and 0.85 rad/sec gave estimated dispersion coefficients of 8, 11, and 26 cm^2/sec, respectively. These data were used to calibrate a dispersion model (discussed later). Model predicted dye concentrations agree well with measured concentrations (see, for example, Figure 12).

.The effects of vertical dispersion on the transport of the soil were tested by adding a known mass (ca. 4 kg) of soil, uniformly and instantaneously, to the surface of the water column for a fixed dispersion. Soil was added to the tank with a louvered aluminum fan shutter (1.3 by 1.3 m) suspended 10 cm above the water surface. Particle mass was intermittently sampled from three 2.5 cm diameter syphon tubes, 1.2, 2.2 and 4.4 m below the water surface. The hydrostatic head of the water column was sufficient to provide flow rates of 0.9 l/sec. Samples (4.0 l) were taken on a log time scale for up to 4 hours after a soil addition.

Particulates were separated from solution by filtration. Particles greater than 63 microns were separated with a sieve, rinsed onto a filter, and total mass for the known volume calculated. The mass of less than 63 micron particles was determined by collecting a 500 ml aliquot of water after passing the sieve, then quantifying the mass retained on passage through a 1 micron filter. The mass per unit volume was calculated and added to the greater than 63 micron fraction to give the concentration of total particulates. Water and particulate samples were collected for radioisotope analysis from the 11 cm^2/sec dispersion experiment. The percentage of mass removal from the water column was calculated by volume weighting the total suspended solids concentration for each sample period, summing for the sample period, and dividing by the known initial mass.

SECTION 3

EXPERIMENTAL RESULTS

SIZE DISTRIBUTION

The grain size of the Middlsex soil ranged from less than 63 microns to greater than 2000 microns. Seventy-five per cent of the mass was measured between 63 and 2000 microns. Cumulative mass fraction versus particle size showed that this sample of Middlesex soil was dominated by sand size particles smaller than 1 mm (Figure 4). The median grain size was approximately 350 microns.

Comparison of bulk sample size classifications between 20 and 600 microns (this range represents 62 per cent of the total mass) by the wet and dry methods indicated that apparently larger sizes were measured with the wet sizing technique (Figure 5). This may have resulted from mechanisms such as particle agglomeration, surface wetting, and swelling from hydration, as well as from differences in the measuring techniques.

Comparision of dry and wet size distribution data for particles from single dry sieving size classes (63-90, 90-106, 106-180, and 180-355 microns) supported the apparent size shifts (Figures 6a-e). This tendancy was less pronounced for the larger size classes than for the smaller size classes.

ACTIVITY DISTRIBUTIONS

Gross estimates for radioactivity (total gamma plus beta or total alpha) indicated significant activity was associated with each size class (Figure 7), but the activity was not uniformly distributed among size classes on a unit mass basis (Table 1). Furthermore, autoradiography of the soils demonstrated the activity was associated with discrete particles. The median in gross activity was found at the 125 micron size Figure 7).

The mass-weighted cumulative activity distributions for individual isotopes were different from the cumulative mass and the cumulative gross activity distributions (Figure 8). The individual isotopes that were measured exhibited higher median sizes for activity than did the measure of gross activity. Ra-226, U-234, U-238, and Th-230 were similar to each other, with median distributions at 250 microns. Pb-210 and Po-210 had higher median distributions, 300 and 600 microns, respectively. Several isotopes, Th-227, Th-228, Th-232, and U-235, did not show consistent cumulative activity distributions due to large counting errors resulting from low activity and small sample sizes.

Less than 10 per cent of the activity was found associated with the silt-clay fraction (less than 63 microns) of the sample (Figure 8). Independent of the method of quantification and isotope of interest, the radioactivity associated with the sample resided in the
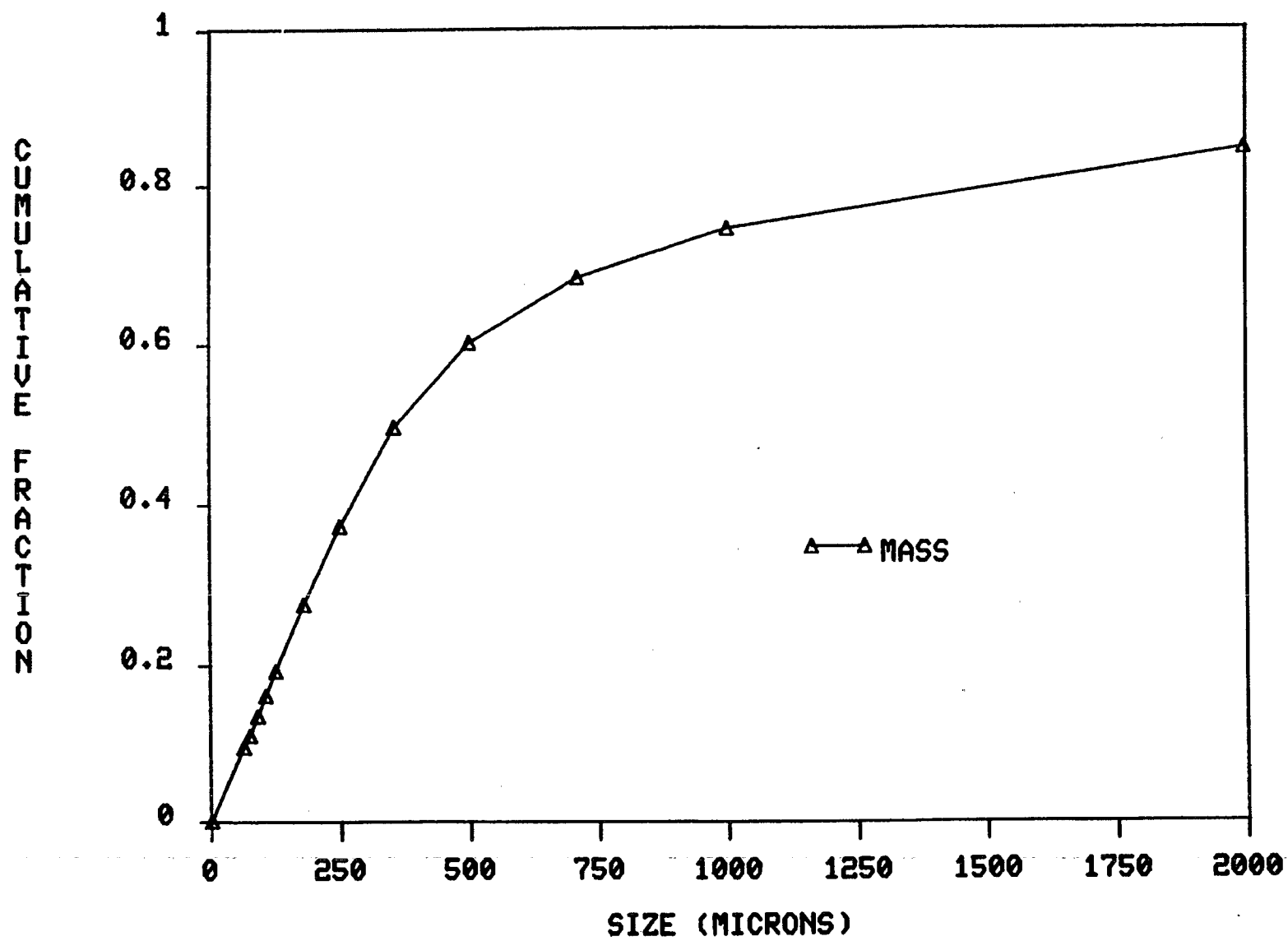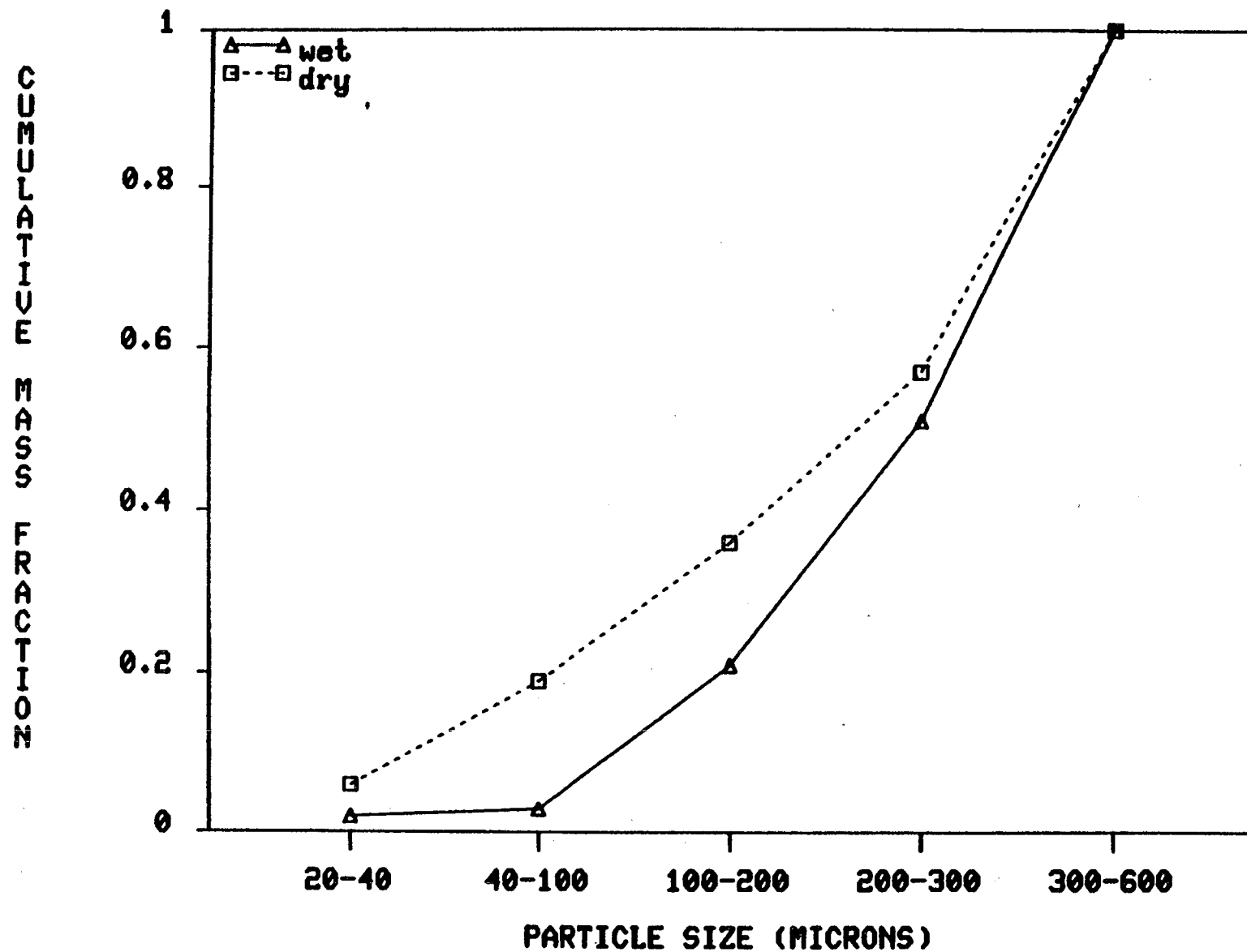
11

Figure 4.   Cumulative mass versus particle size.

Figure 5. Size distribution between 20 and 600 microns as determined by
wet and dry methods.

14

MASS FRACTION

1

0.8

0.6

0.4

0.2

0

| wet |
| dry |

20-40   40-100   100-200   200-300   300-600
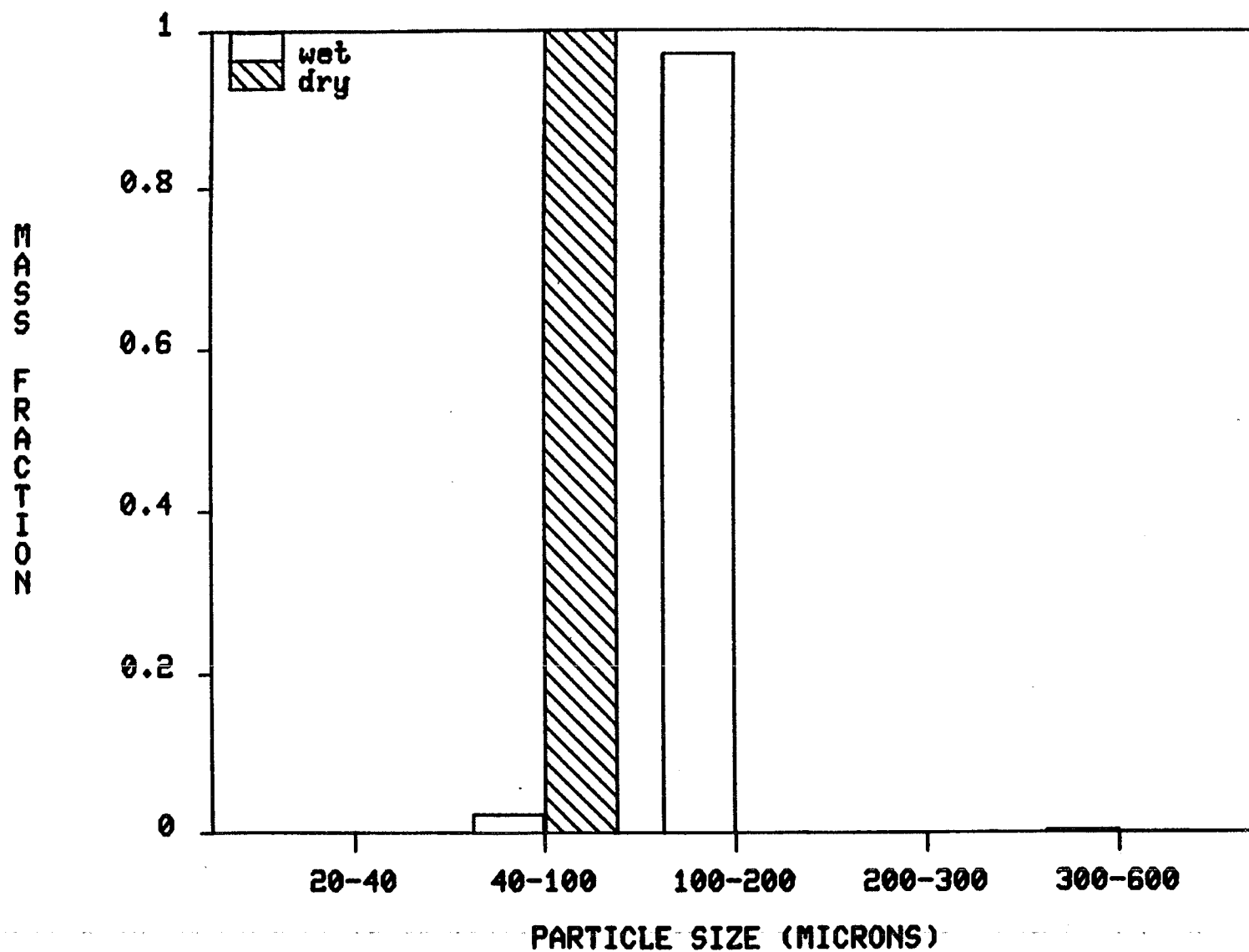
PARTICLE SIZE (MICRONS)

Figure 6. Size distributions of particles separated into size classes by dry sieving, as determined by wet and dry methods. (a) 63-90 micron size class.
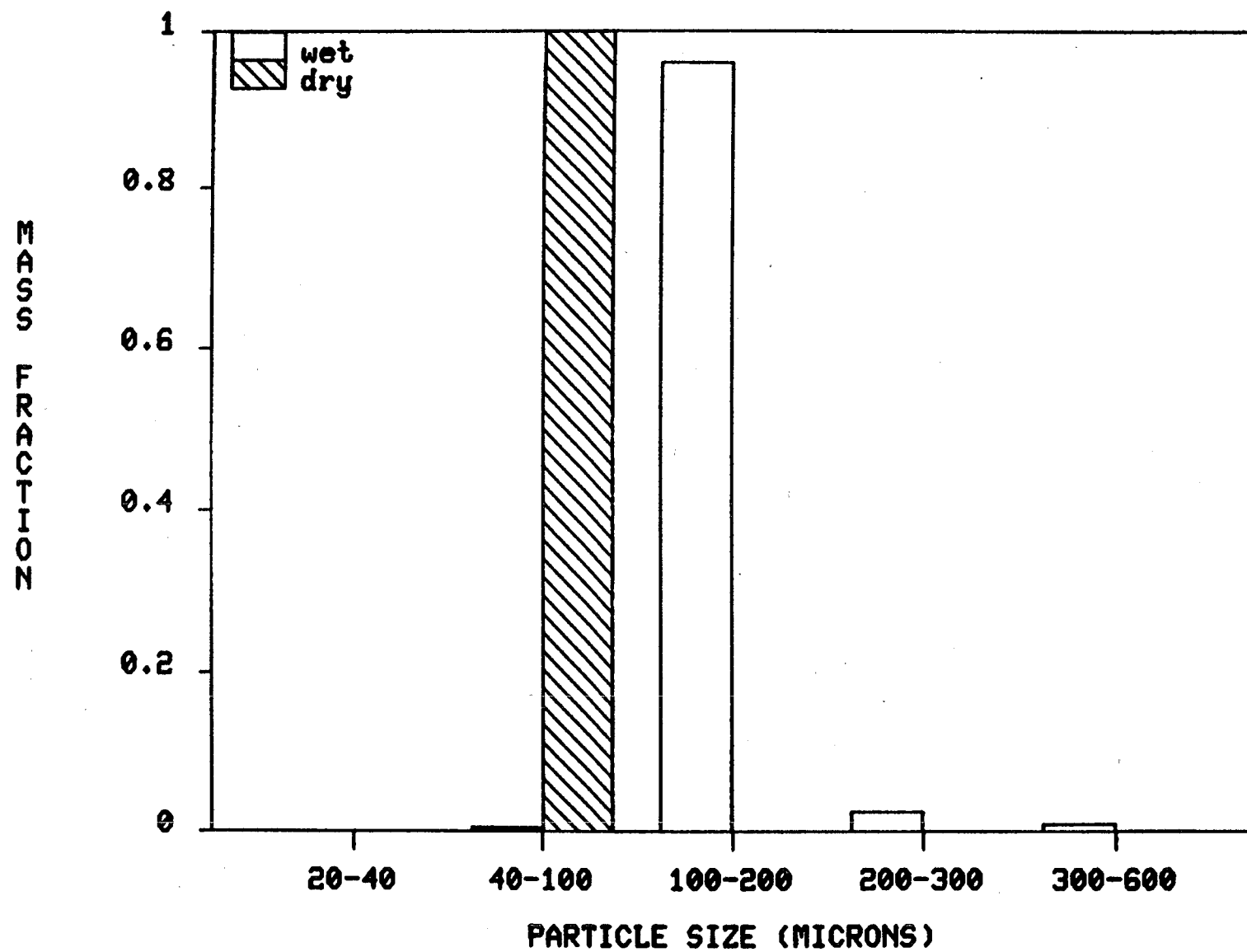
Figure 6b.   90-106 micron size class.

Figure 6c.   106-250 micron size class.

MASS FRACTION

1

0.8

0.6

0.4

0.2

0

wet
dry

20-40   40-100   100-200   200-300   300-600

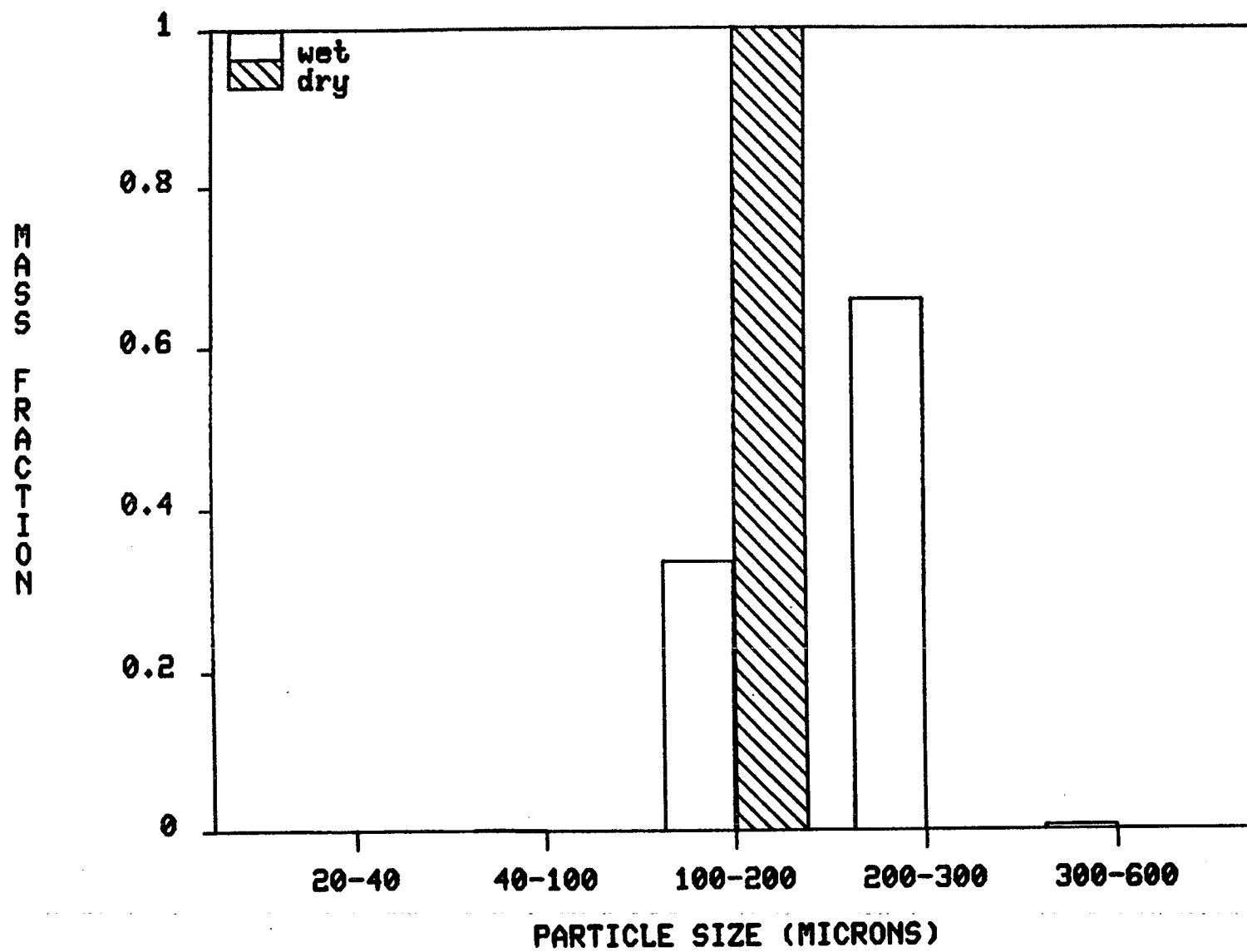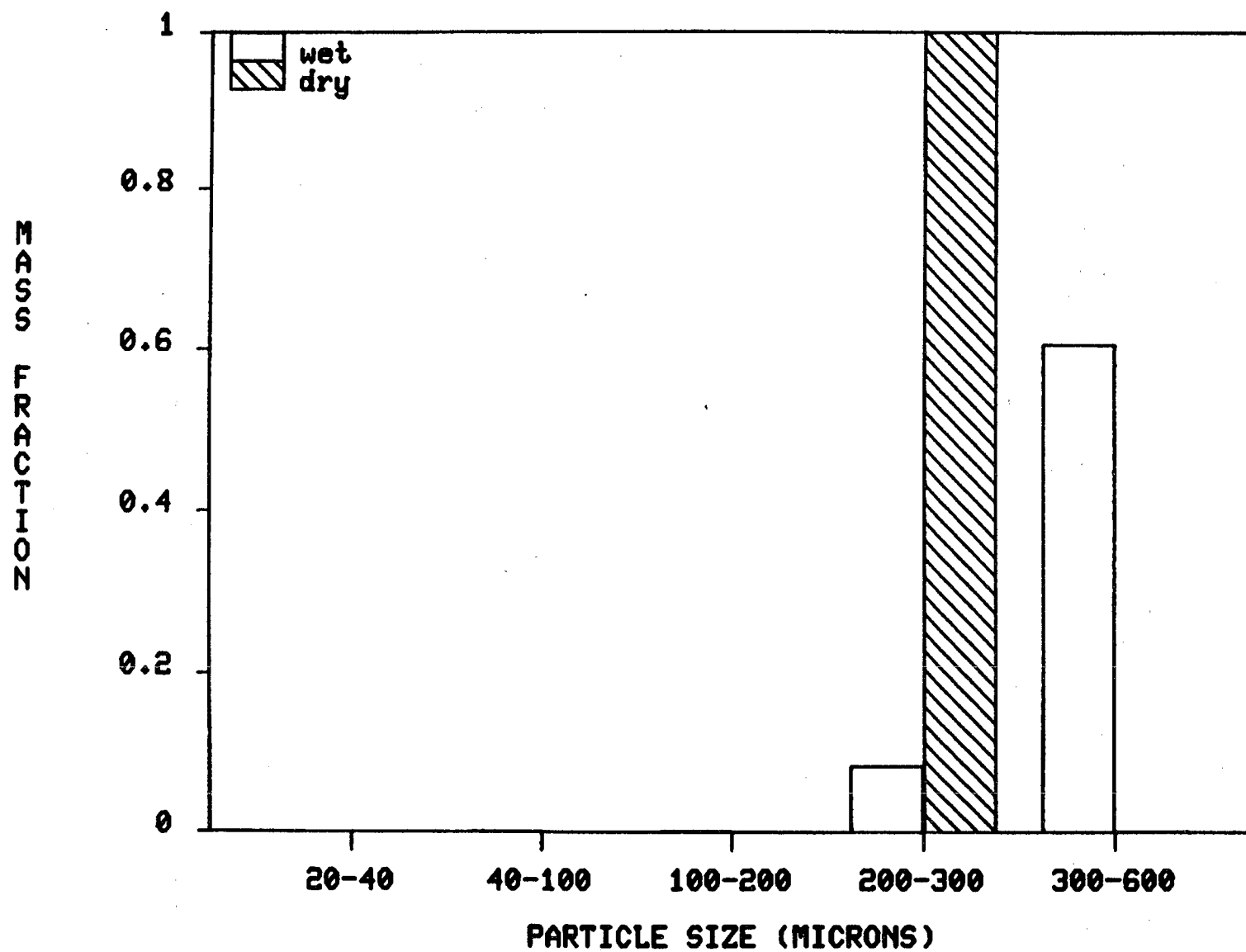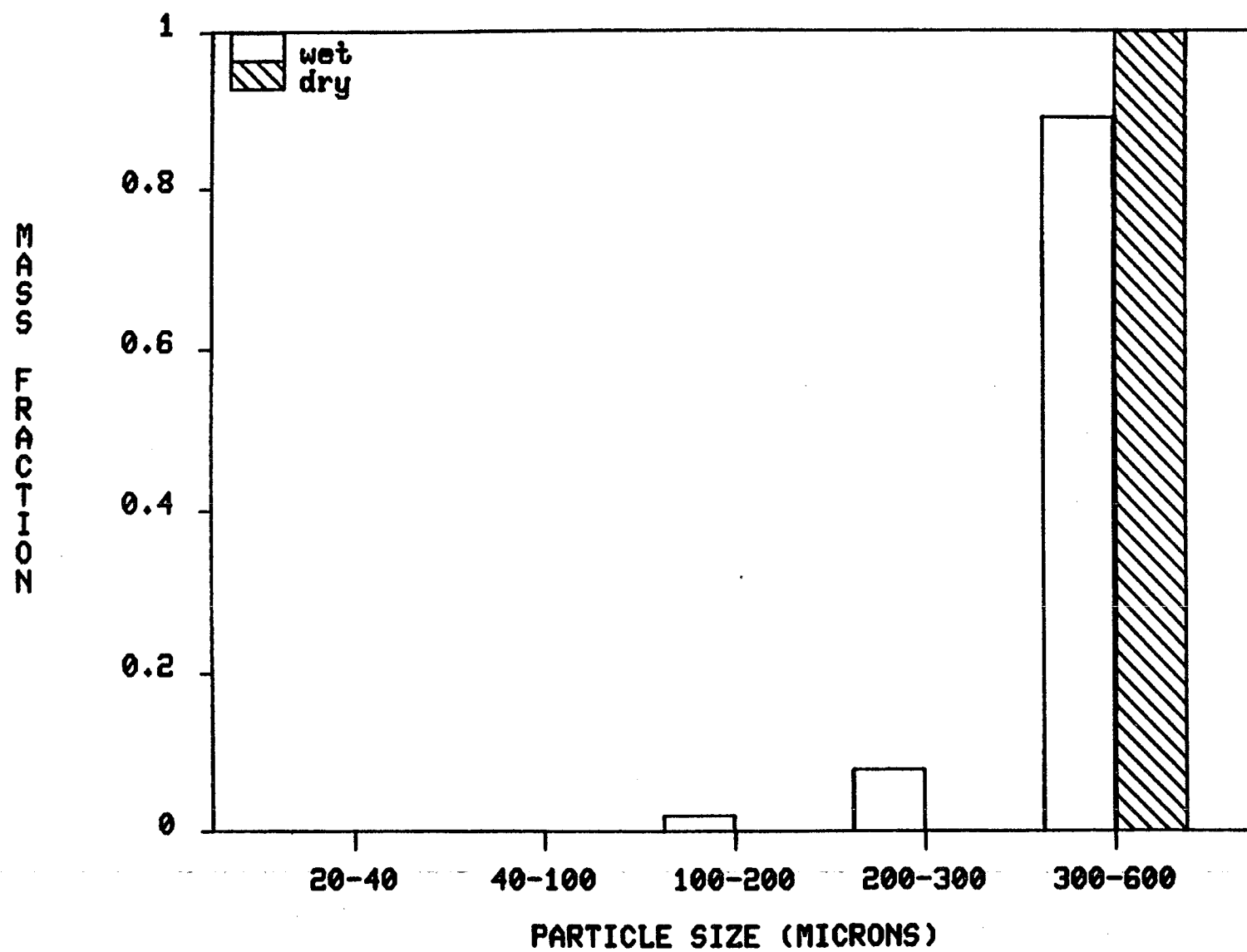PARTICLE SIZE (MICRONS)

Figure 6d.   250-355 micron size class.

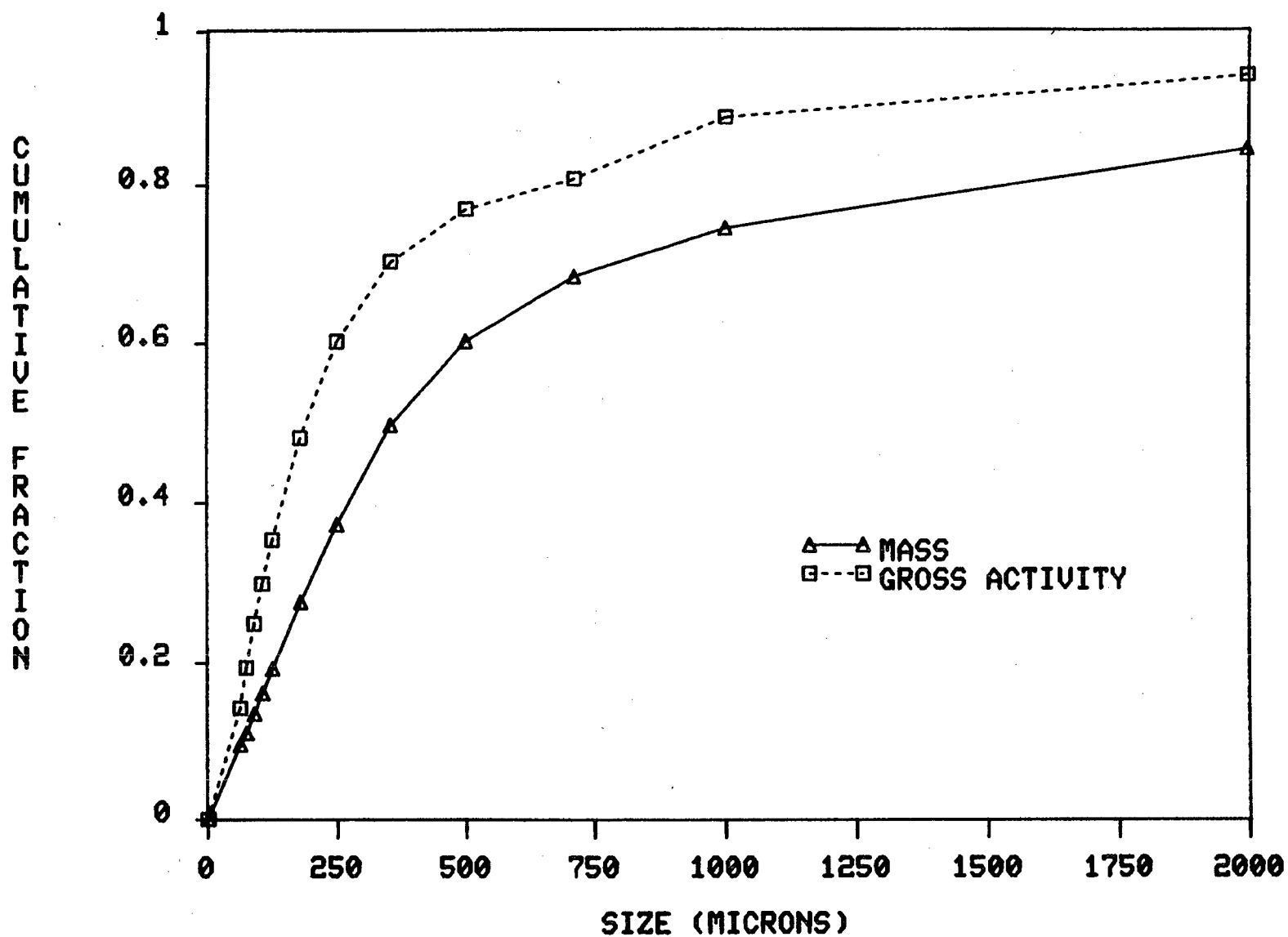Figure 6e.   355-600 micron size class.

Figure 7.   Cumulative gross activity versus particle size.

TABLE 1. RADIOISOTOPE ACTIVITY FOR MIDDLESEX SOIL**

Particle Diameter+	Ra-226 2-3*	Pb-210 14-41*	Po-210 7-12*	U-234 12-16*	U-235 17-49*	U-238 12-16*	Th-227 26-62*	Th-228 10-218*	Th-230 6-15*	Th-232 8-69*
<63	50.3	56.0	57.2	49.2	4.6	49.1	4.3	7.0	54.9	8.2
63	8.6	8.4	8.4	9.7	3.8	9.7	0.7	1.1	10.2	1.2
75	14.2	19.1	13.4	11.4	2.3	11.8	0.9	1.3	11.2	1.5
90	15.1	16.4	13.7	17.3	0.8	16.2	1.0	1.6	15.2	1.3
106	13.6	14.9	15.9	14.8	1.8	14.0	1.1	1.5	13.5	1.7
125	59.3	61.5	52.9	65.4	2.4	63.9	3.9	4.2	57.9	47.9
180	28.5	27.7	37.7	26.6	1.1	28.1	2.3	1.9	31.6	2.0
250	24.9	29.9	27.2	30.1	1.8	28.5	1.7	0.9	21.7	1.3
355	20.8	19.9	19.3	14.2	0.7	15.2	1.2	0.5	16.6	1.3
500	18.8	29.2	20.0	24.8	1.1	24.7	2.2	<0.1	23.5	1.3
710	17.3	32.5	26.3	35.1	1.9	33.5	22.1	0.3	31.6	0.3
1000	58.3	149.3	64.7	53.7	2.2	56.2	9.7	52.9	84.4	76.0
>2000	29.1	49.6	31.8	24.1	0.9	22.2	3.2	<0.1	31.9	1.3
Total	358.8	514.5	388.3	376.5	25.5	373.2	54.2	73.1	404.1	145.2

+ Particle diameter in microns. Particles separated by standard sieves.

* Per cent counting error specified as two standard deviations.

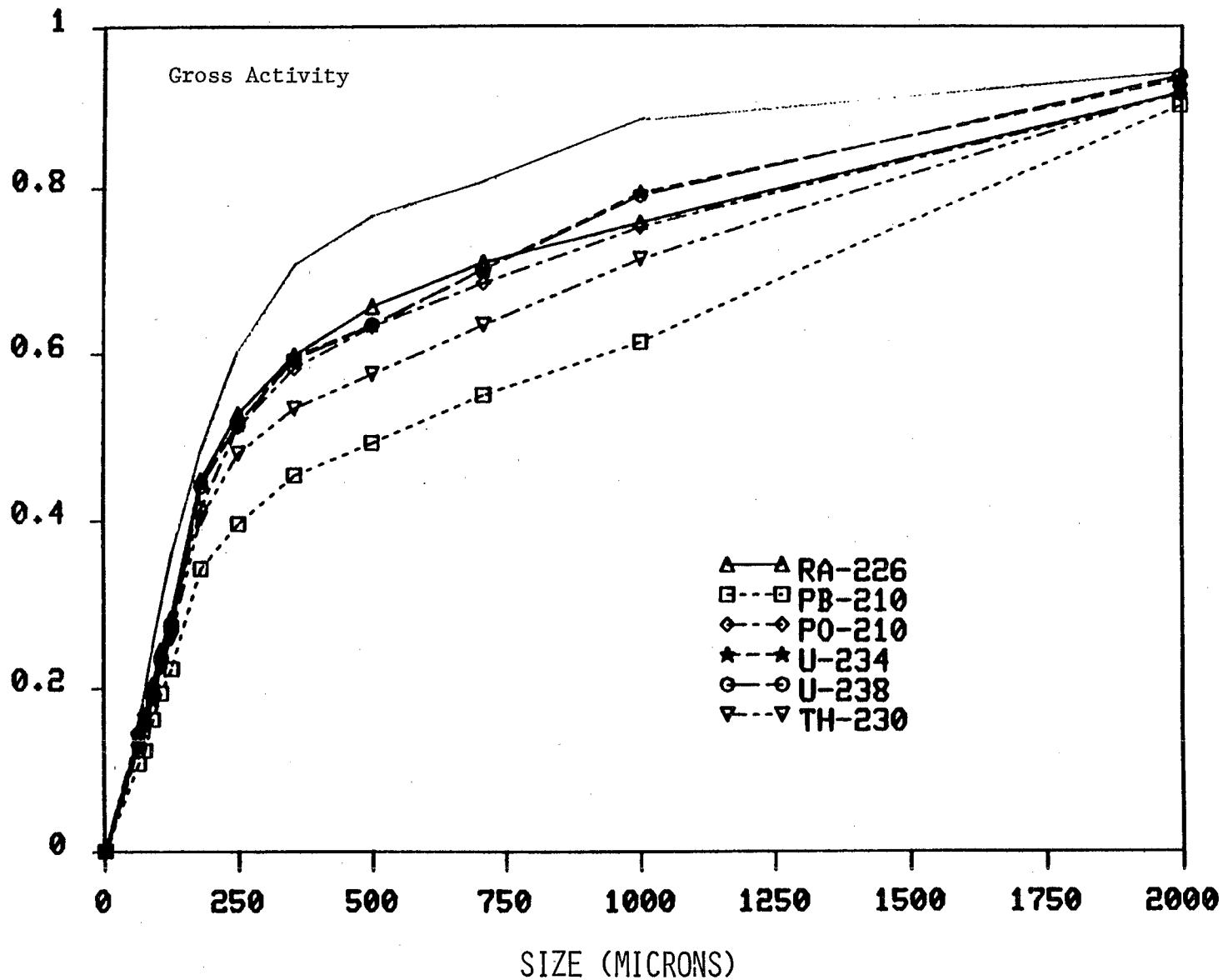** Activity express in pCi/g times mass fraction in that sieve size (g/g).

Figure 8. Cumulative individual isotope activity versus particle size.

larger sand size particles. Therefore, with the exception of the fraction of the isotopes mobilized to the dissolved phase, transport of the isotopes should be described by processes controlling the transport of sand size and larger particles.

ISOTOPE DISSOLUTION

Partition coefficients (Kd) for the individual isotopes ranged between 10^3 and 10^6 (Table 2), depending on the isotope. The isotopes which undergo the most mobilization to the dissolved phase are Ra-226 and the uranium isotopes. Based on these experiments, 20 to 24 percent of these isotopes may be converted to the soluble phase within 20 hours of initial contact with sea water. Considering the small sample size, sandy texture, association of activity with discrete particles in these samples, and counting errors, it seems likely that these estimates may not accurately represent the dissolution which may have been expected from these soils. Mass balance considerations from the mesocosm transport studies suggested that 10 percent of the uranium and Ra-226 may be released to the dissolved phase while less than 1 percent of the Po, Th and Pb will be solubilized over periods of hours to days (Table 3). Dissolution over time scales up to 3 months are being examined using mesocosm studies (Hunt, 1986). These results suggest that most of the radioactivity (90 percent) will remain associated with the soils as they are transported through the water column.

SETTLING VELOCITY DISTRIBUTIONS

Soil settling velocities were determined for a series of undried composite Middlesex samples and a series of selected size classes which had been dried. Reproducibility between runs of a given sample was good. An example of the results from a typical experimental run is shown in Figure 9. (See Appendix A for data from all of the experimental runs.) A significant fraction (20 per cent) of the composite sample settled at greater than 5 cm/sec in the upper 16 cm of the column. However, the fraction of particles descending past 39, 62, and 85 cm at velocities greater than 5 cm/sec decreased to 10 per cent. The momentum from the actual soil addition could have resulted in the observed decrease. Other causes may be theorized for this observed shift, such as wetting or hydration of particles and disaggregation of soil clumps. Regardless of the cause, the shift to a slower velocity reached an equilibrium at 39 cm.

Minimum settling velocities for the composite sample increased from 0.2 cm/sec at 16 cm to 1.3 cm/sec at 85 cm. The median settling velocity followed a similar trend. The observed velocity distribution shift suggested by these data had not reached an equilibrium state by 85 cm. Possible causes for this observed shift include wetting or hydration of particles and agglomeration of soil particles.

Settling velocity distributions for individual size classes also increased on passage through the sea water (Figure 10a-e), particularly in the smaller size classes. The changes in settling

TABLE 2.   ISOTOPE SOLUBILITY AND PARTITION COEFFICIENTS FOR MIDDLESEX SOIL

Suspended solids	270 mg/kg			280 mg/kg			900 mg/kg			1220 mg/kg		
	KD+	per cent soluble	error*	KD+	per cent soluble	error*	KD+	per cent soluble	error*	KD+	per cent soluble	error*
Ra-226	8.98×10^3	28	1	4.43×10^3	44	1	3.84×10^3	22	.7	4.37×10^4	2	2
Pb-210	1.37×10^5	2.5	70	1.38×10^5	2.5	91	7.11×10^5	1.5	70	1.82×10^5	0.4	119
Po-210	3.99×10^5	0.9	29	2.08×10^5	1.6	20	5.09×10^5	0.2	30	2.77×10^5	0.2	21
U-234	9.59×10^3	27	9.5	1.33×10^4	21	13	4.34×10^3	19	13	4.95×10^3	14	14
U-235	1.16×10^4	24	19	1.10×10^4	24	21	4.34×10^3	20	15	3.44×10^3	19	16
U-238	9.11×10^3	28	9.5	1.42×10^4	20	13	4.53×10^3	19	13	4.74×10^4	14	14
Th-227	9.18×10^4	3.7	62	1.20×10^4	2.8	77	7.41×10^4	1.5	65	5.44×10^4	1.5	51
Th-228	5.78×10^4	5.8	34	4.46×10^5	7.2	32	2.83×10^5	3.7	26	3.82×10^5	2.0	31
Th-230	1.26×10^6	0.3	35	8.50×10^6	0.4	33	9.91×10^7	0.1	36	9.55×10^6	<0.1	34
Th-232	1.19×10^6	0.3	140	1.63×10^6	0.2	140	2.86×10^7	<0.1	2500	2.85×10^6	<0.1	300

+ Partition coefficient (kg seawater/kg particulate).

* Per cent counting error specified as two standard deviations.

TABLE 3. MASS BALANCE ESTIMATES OF ISOTOPE SOLUBILITY FOR MIDDLESEX SOIL FROM MERL MESOCOSM EXPERIMENTS

ISOTOPE	TOTAL ADDED (pCi)	TOTAL SOLUBILIZED* (pCi)	PERCENT SOLUBILIZED
Ra-226	1676	120	7.2
Pb-210	1734	18	1.0
Po-210	1593	21	1.3
U-234	1584	135	8.5
U-235	44	6	13.6
U-238	1562	132	8.5
Th-227	119	0.62	0.5
Th-230	1804	1.7	0.09
Th-232	1848	1.3	0.07

* After 4 hours of exposure.
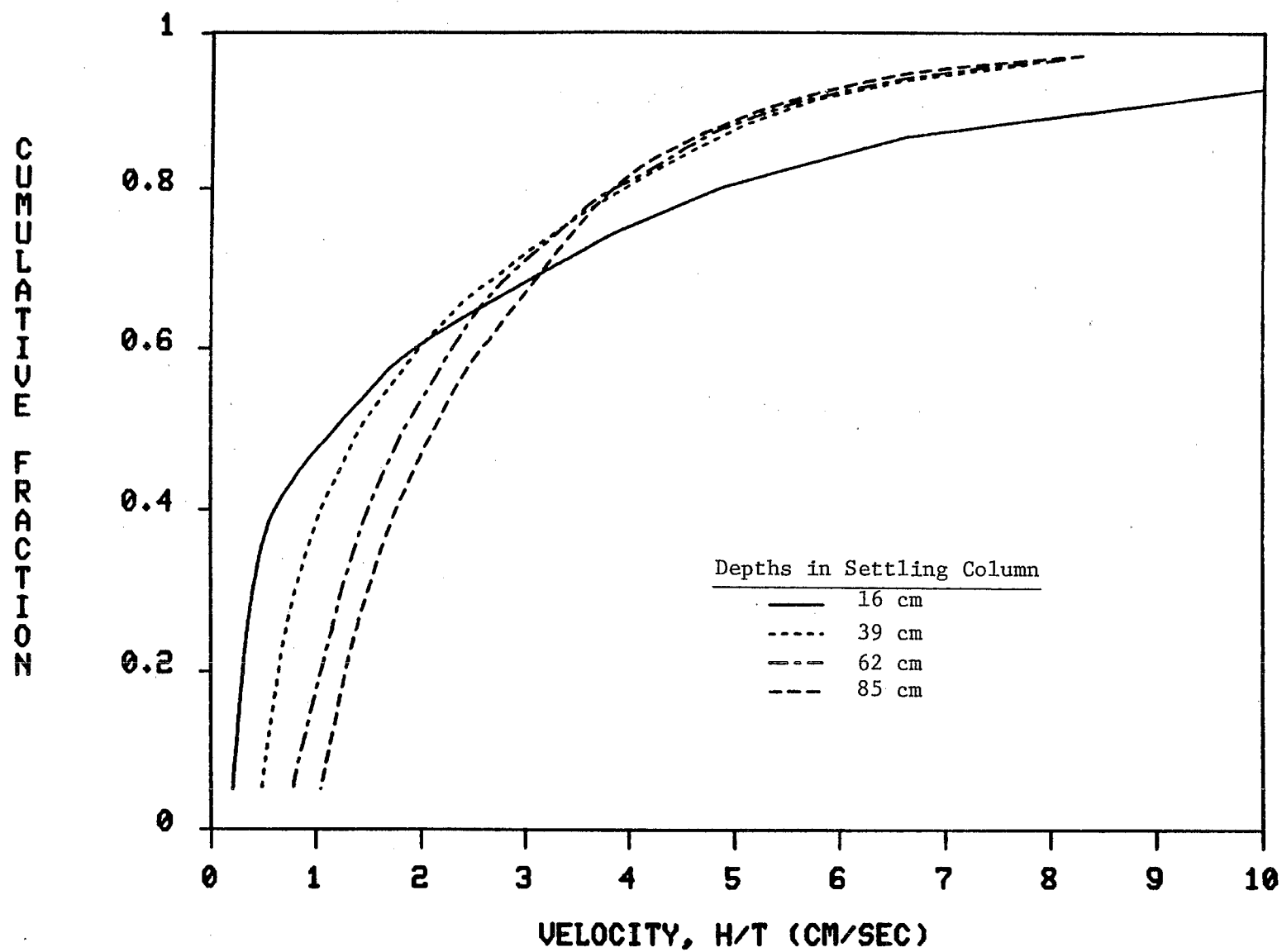
Figure 9. Settling velocity distribution for Middlesex soil determined from laboratory column experiments.
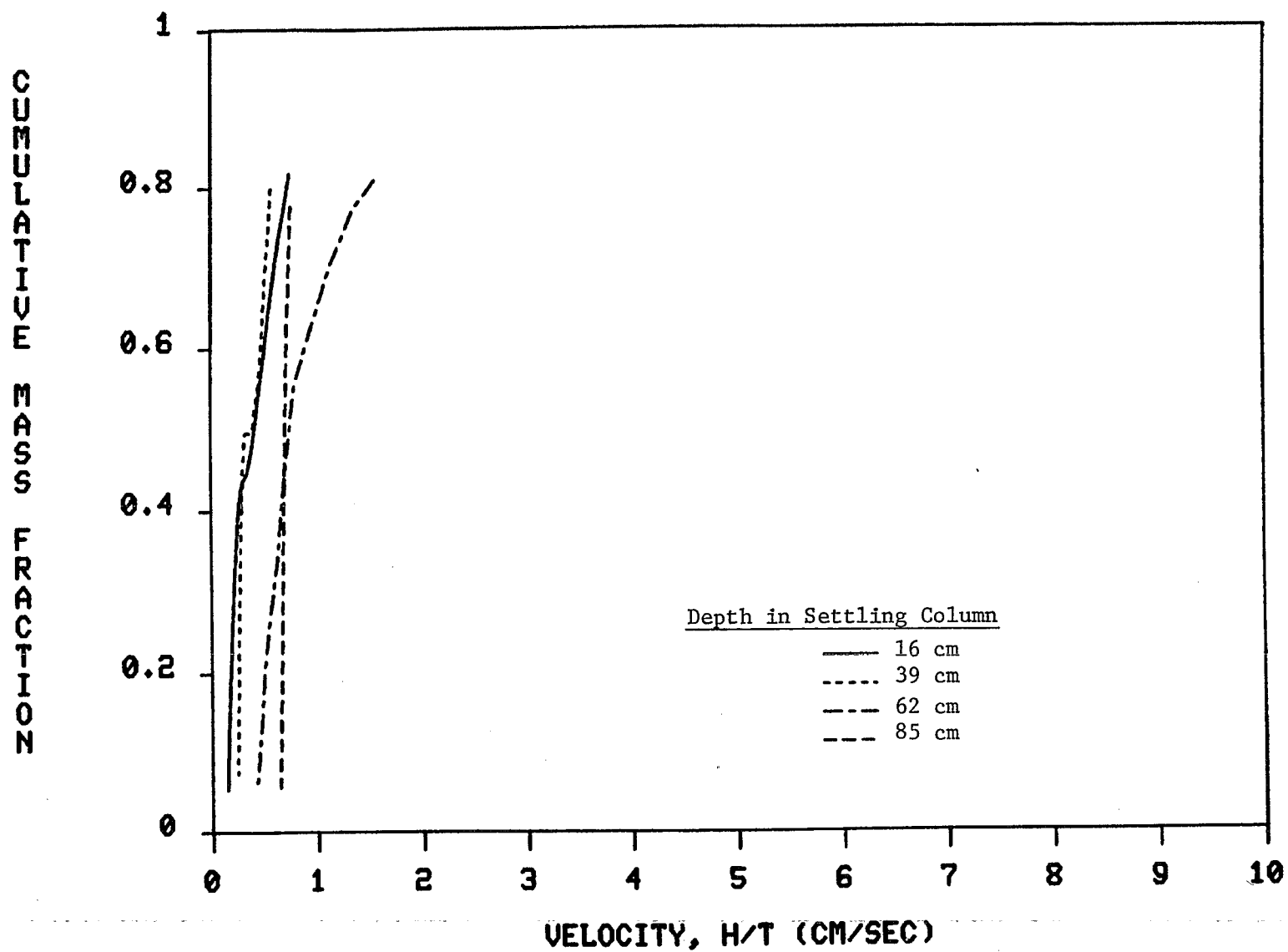
Figure 10. Settling velocity distributions for Middlesex soil separated into size classes by dry sieving. (a) 63-90 micron size class.
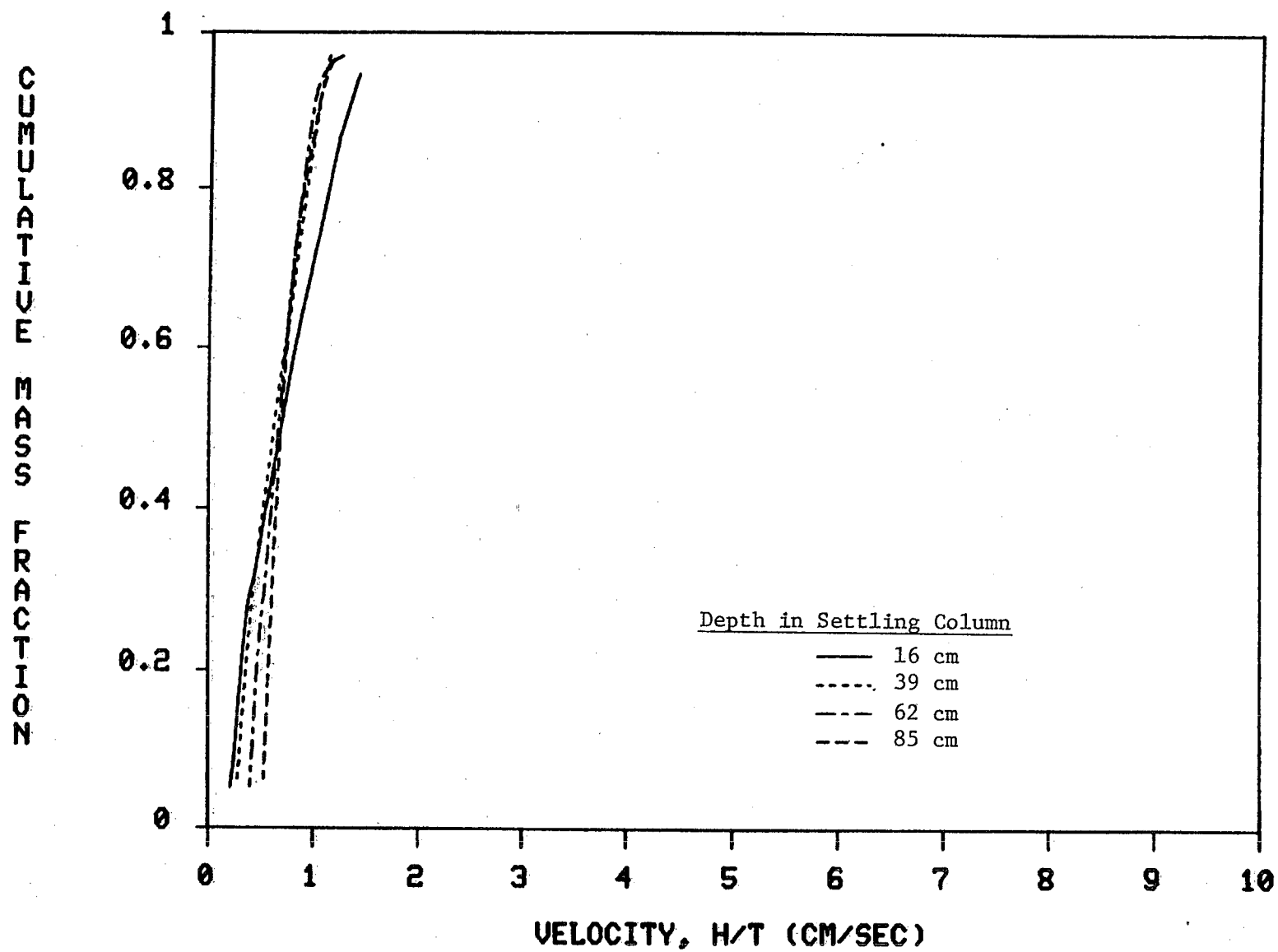
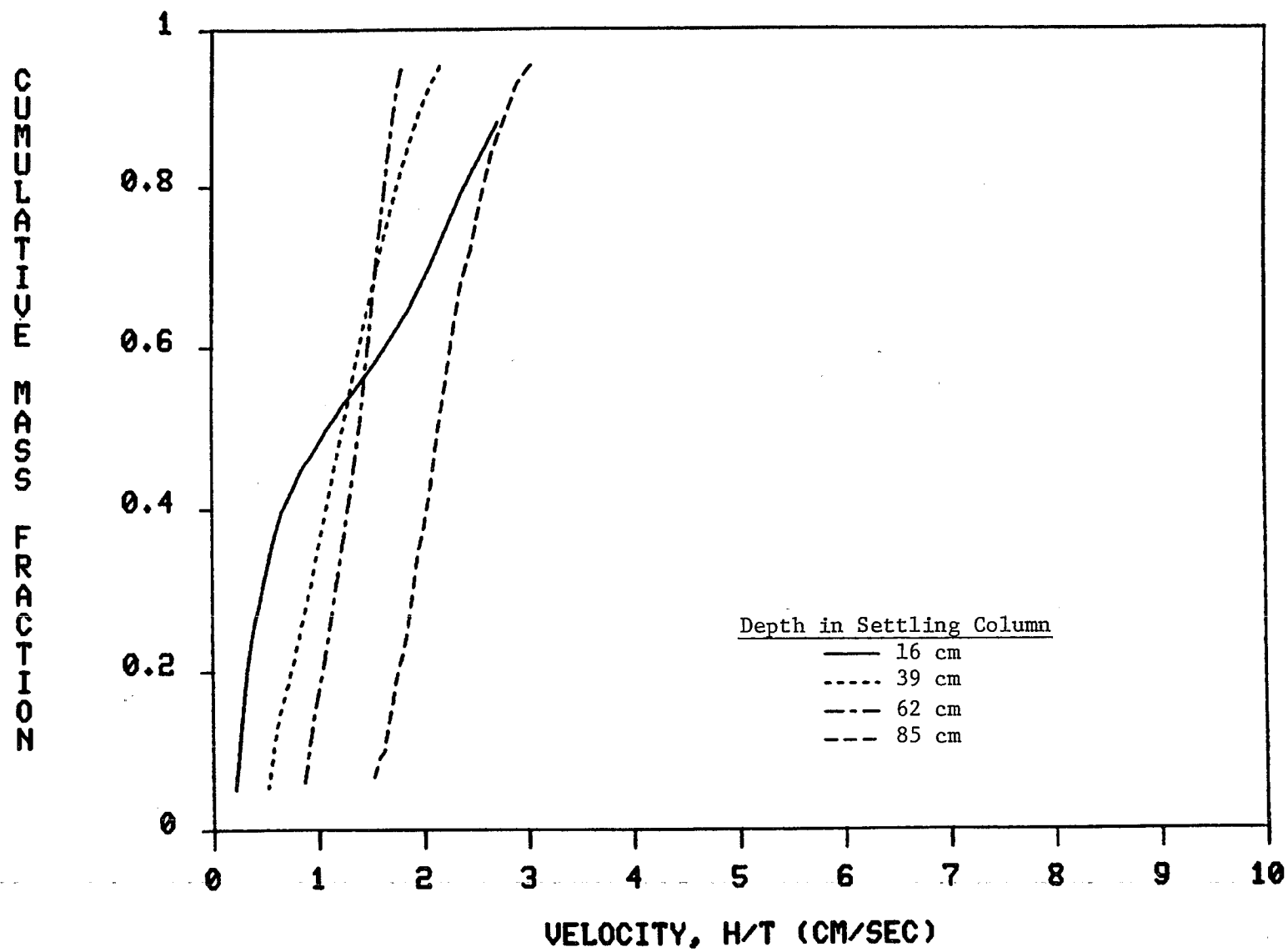Figure 10b.   90-106 micron size class.

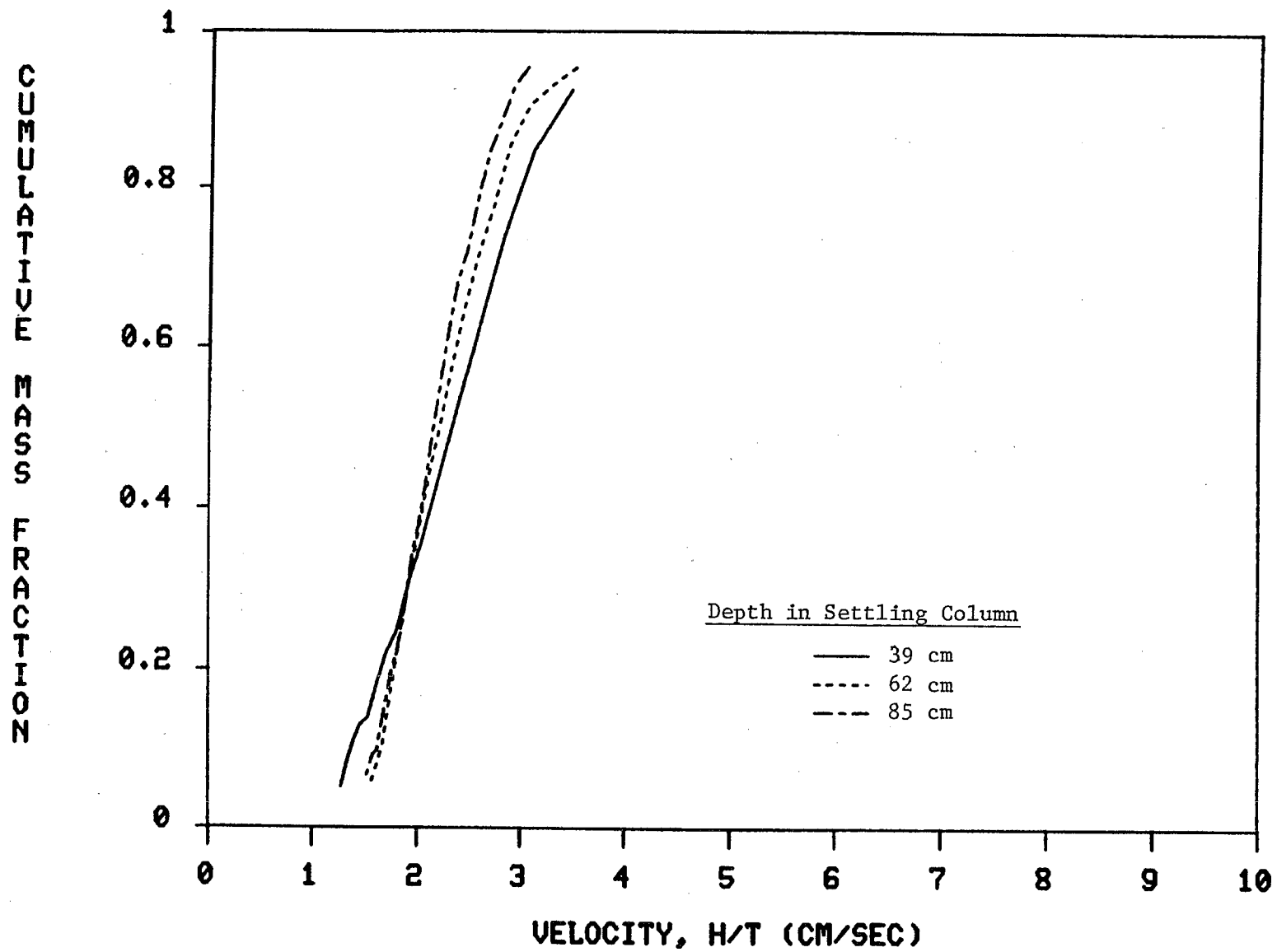Figure 10c.   106-250 micron size class.

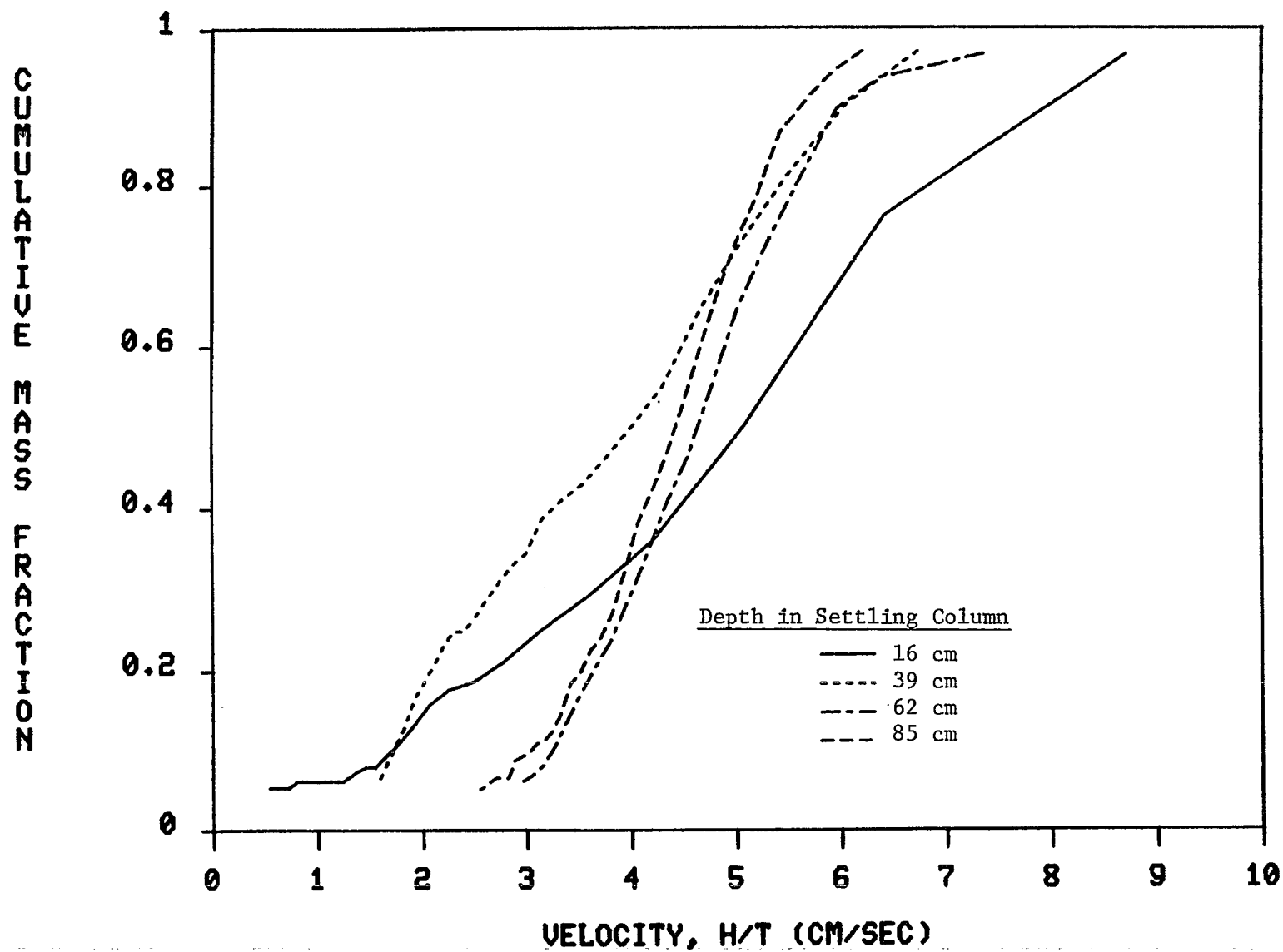Figure 10d.   250-355 micron size class.

Figure 10e.   355-600 micron size class.

velocity distributions at the four transmissometer depths indicated
that an equilibrium state had not been reached by 85 cm for the three
smaller size classes.

The settling column results indicated that the Middlesex soil
will fall rapidly through the water column, and that changes in
settling velocity distribution would occur upon introduction into sea
water. Whatever the mechanism for the observed change, the increased
velocities act to reduce the water column residence time for the finer
particles. The velocity distributions approached an equilibrium state
within very short vertical distances, particularly relative to the
depth at a deep-ocean disposal site.

MESOCOSM-SCALE EXPERIMENTS

The effects of vertical dispersion on the transport of the soil
in the mesocosm tank was difficult to determine. The rapid descent of
the particles in the MERL mesocosm limited the quality of data.
Approximately 4 seconds was required per sampling to obtain the 4.0
liters used to determine the solids concentration. A peak in mass
descent through the water column was not detected during the
experiments (see Figure 11). The peak in mass was most probably
between ports for the initial samplings. We were able to estimate
the total mass of particles remaining in the mesocosm as a function
of time to determine the mass removal from the water during the
experiments. These results (Table 4) suggest changes in dispersion
influenced the mass removal in the 5 m MERL water column, with
higher dispersion increasing the mass residence time. Differences
in mass removal at different dispersions could be accounted for by an
analytical expression relating gravitational settling, V, and vertical
diffusion, D (Table 4). Extrapolating this analytical expression to
a 4000 meter water column suggests that the dispersion levels, as
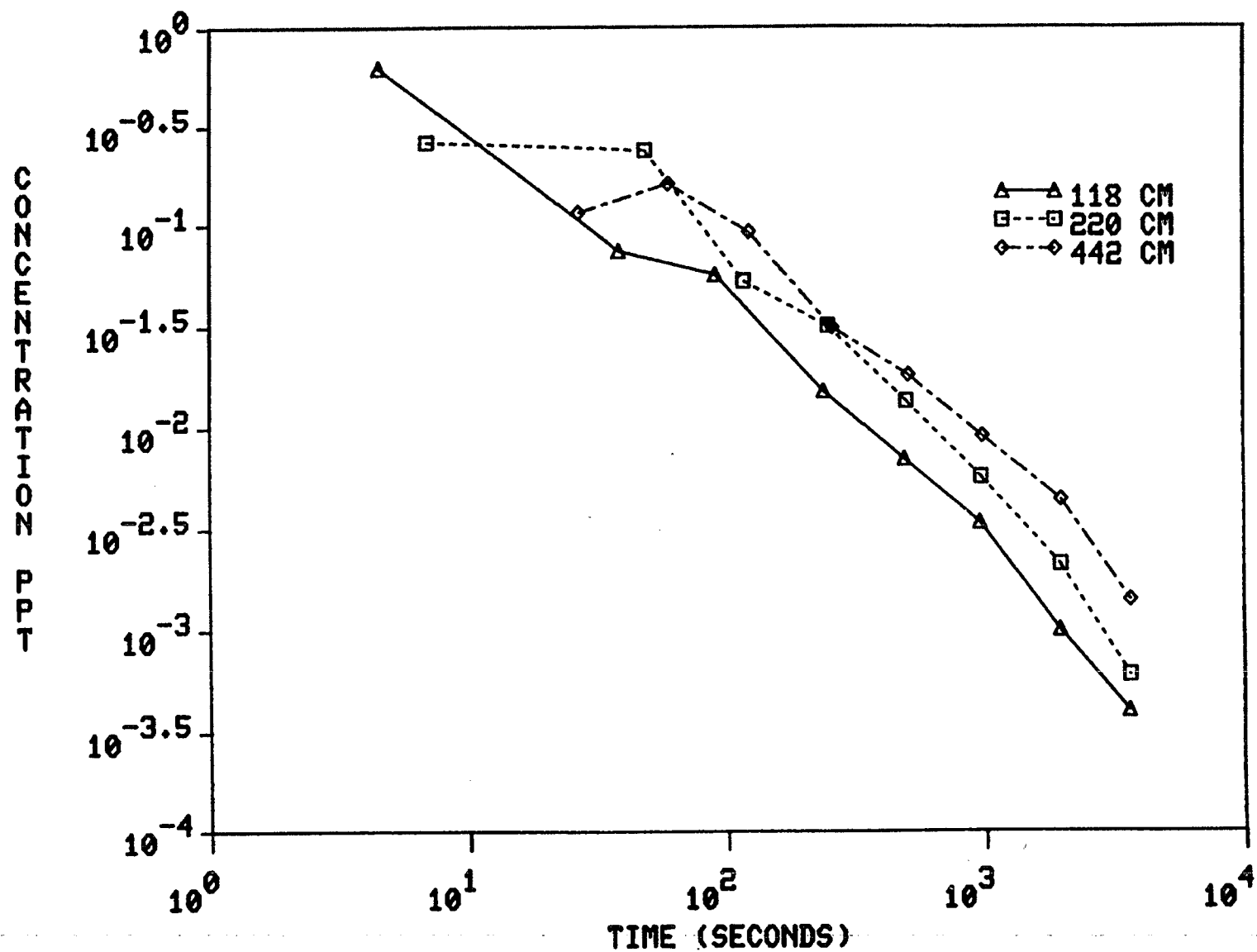used in the MERL tank, would modify mass removal times by less than
five per cent.

31

Figure 11. Mass removal experimental results for particles greater than 63 microns and with 11 cm^2/sec dispersion in MERL mesocosm.

TABLE 4. EFFECTS OF DISPERSION ON MASS REMOVAL OF MIDDLESEX SOIL
FROM MERL MESOCOSM EXPERIMENTS

| | Dispersion | | | |
| | 11 cm^2/sec mixing | | 26 cm^2/sec mixing | |
per cent mass removed	t+ (sec)	V* (cm/sec)	t+ (sec)	V* (cm/sec)
50	94	5.3	78	6.4
84	229	2.5	363	1.7
90	385	1.6	611	1.2
95	1322	.59	2543	.43

+ Estimated by volume weighting concentrations for a sampling period, and linearly extrapolating between sampling periods.

* V is estimated from mass removal time by the following expression (derived from results in Csanady, 1973):

$$X = 0.5 \ [erf((b-Vt)/(2 \ \sqrt{Dt})) + erf((b+Vt)/(2 \ \sqrt{Dt}))],$$

where

X = fraction remaining in water column,
$erf(\ )$ = error function,
b = depth of water column,
V = settling velocity,
t = time for removal, and
D = vertical diffusion.

SECTION 4

MODELING APPROACH

MODEL DEVELOPMENT

Particulate matter is vertically transported through the water column by a combination of convection, settling, and diffusion (both turbulent and molecular) processes. The model used here assumes that vertical convection of the fluid was not a significant transport process. It has been shown that vertical convection is only significant in large water bodies where strong upwelling and downwelling occur, e.g., in nearshore coastal regions, while settling and diffusion are ubiquitous phenomena (Lick, 1982). Two different levels of models were considered to describe vertical transport of non-interacting particles. Level 1 assumed the particles can be characterized by a single average particle size and an associated average settling velocity. The Level 1 particles will be referred to as monodispersed. Level 2 assumed the particles can be treated as a system of independent, or non-interacting, size classes, each with its own characteristic settling velocity. Level 2 particles will be referred to as polydispersed.

Level 1

The one-dimensional, time-dependent, convective-diffusive transport model presented here involved two vertical transport terms, settling and diffusion. The settling term for non-interacting, single-sized particles was the mean settling velocity of the material relative to the fluid, V (the velocity of the fluid, Vf, minus the particle fall velocity, Vp), multiplied by the concentration:

$$\frac{\partial C}{\partial t} = - \frac{\partial VC}{\partial z} , \qquad (1)$$

where C is the particle concentration, z is depth, and t is time. The particle fall velocity, Vp, was expressed as a function of particle diameter for three different Reynolds number regimes (Weber, 1972):

Stokes settling (Re < 1):

$$Vp = \frac{g}{18\mu} (\rho_p - \rho_o) D^2 , \qquad (2)$$

34

Transitional settling (1 < Re < 1000):

$$V_p = \frac{0.72 \, (\rho_p - \rho_0) \, D^{1.6}}{\rho_p^{0.4} \, \mu^{0.6}} \quad , \qquad (3)$$

Newton's settling (1000 < Re < 25000):

$$V_p = 1.82 \sqrt{\frac{(\rho_p - \rho_0) \, D \, g}{\rho_0}} \quad , \qquad (4)$$

where Re is the Reynolds number based upon particle diameter $(D\rho_0 V_p/\mu)$, g is gravitational acceleration, μ is viscosity of the fluid, ρ_p is particle density, ρ_0 is fluid density, and D is particle diameter. Alternatively, Vp was determined from laboratory settling column experiments.

The vertical diffusion was a combination of the vertical eddy diffusivity coefficient, Dv, and the molecular diffusion coefficient, Dm,

$$\frac{\partial C}{\partial t} = \frac{\partial}{\partial z} (D_v + D_m) \frac{\partial C}{\partial z} \quad . \qquad (5)$$

The equation for the first level vertical transport model was the combination of Equations (1) and (5),

$$\frac{\partial C}{\partial t} = \frac{\partial}{\partial z} (D_v + D_m) \frac{\partial C}{\partial z} - \frac{\partial V C}{\partial z} \quad , \qquad (6)$$

The boundary conditions used with Equation (6) were that (1) the upper boundary was treated as a surface with no net mass flux across it, and (2) the bottom boundary was treated as an adsorptive boundary, i.e., particles that reach this boundary "stick" to it. The initial condition was specified as having the entire mass of soil particles in the surface water layer, i.e. the particles were considered to be added instantaneously to the surface at time t = 0.

There are several assumptions that govern our use of Equation (6). These are:

1. The horizontal variation in concentration was negligible.

2. Mixing was accounted for by a constant eddy diffusivity.

3. There was no hindered or non-discrete settling of particles due to hydrodynamic influences.

4. Vertical convective fluid transport was insignificant, i.e., $V_f = 0$.

5. The particle size distribution was treated as a single-size category characterized by an average particle size with an average settling velocity.

6. The particles formed a stable suspension, i.e., no coagulation occurred.

Level 2

Most particulate systems, including the Middlesex soil, are not monodispersed suspensions. Under the condition where assumption (5) above is not valid, a system of equations must be employed, each similar to Equation (6). Each equation would correspond to a single size category. The Level 2 modeling approach assumed that several state variables, one for each representative size or velocity category, could be used to describe the vertical convective-diffusive transport of the polydispersed suspension.

In addition to the assumptions for the Level 1 model, there was an additional assumption for the use of the Level 2 convective-diffusive model. This assumption pertained to the dynamic behavior of the size distribution. It was assumed that the particles neither coagulate and form larger particles nor break-up and form smaller particles. This assumption is only valid for stable, non-coagulating systems that are approaching or have reached a particle size distribution equilibrium, i.e., the particle formation and break-up balance.

A system of partial differential equations was used to describe the vertical transport of the polydispersed particles. This system is:

$$\frac{\partial C_i}{\partial t} = \frac{\partial}{\partial z}(D_{vi} + D_{mi})\frac{\partial C_i}{\partial z} - \frac{\partial V_i C_i}{\partial z}, \quad i = 1, \ldots N, \quad (7)$$

where C_i is the particle concentration in a size category i; V_i, D_{vi}, and D_{mi} are the mean settling velocity, vertical eddy diffusivity coefficient, and molecular diffusivity coefficient, respectively, for size category i; and N is the number of size categories. Boundary conditions and the initial conditions were similar to those used for the Level 1 model. The equations within the above system are not coupled as they would be for a coagulating suspension of particles,

36

i.e., for a dynamic particle size distrbiution. Therefore, the
equation for each size category was solved independently.

MODEL CALIBRATION AND DATA SYNTHESIS

The calibration of the dispersion model, Equation (5), was
conducted to quantify the vertical dispersion in a MERL tank. This
calibration was based on the data obtained during the dye studies.
Figure 12 shows an example of predicted model output superimposed onto
a plot of the observed data. The model output, with vertical
dispersion at 11 cm^2/sec, agrees well with observed data from the
dye study conducted at a mixing speed of 0.52 rad/sec. Similar
agreement was obtained for each mixing level in the MERL tank. The
results of the other experiments appear in Appendix B.

Because the results of the laboratory bench scale experiments
indicated that the soil settling could be treated not as a single
settling velocity but as a distribution of settling velocities, we
applied the Level 2 modeling approach to synthesize the data and to
make model projections for the deep-ocean environment. The convection
terms for the Level 2 system of equations were determined empirically
from the data obtained from the settling column experiments. These
data represent settling velocity distributions for the polydispersed
suspension of soil particles.

The velocity distributions actually used in the model were those
measured at the greatest depth in the experimental settling column (85
cm). Apparent equilibrium was approached at this depth for the
settling velocities in the laboratory system. The equilibrium size
distribution assumption is, therefore, quite reasonable for the
projections to the deep-ocean environment. The size distribution of
the settling particles in the deep-ocean environment would reach an
equilibrium condition before descending through a significant fraction
of the total depth (4000 m). This equilibrium would occur, if for no
other reason, due to reduced particle-particle interaction caused by
simple particle number dilution as a result of the turbulent
dispersion and differential gravitational settling.

MODEL APPLICATION

The Level 2 convective-diffusive model was applied assuming
conditions that would exist at a hypothetical deep-ocean disposal site
in 4000 m of water. The model was used to estimate the soil particle
residence time in the water column and the distance along the
direction of mean flow to deposition on the bottom sediments. An
empirically determined settling velocity distribution and assumed
vertical dispersion, ranging from 0 to 100 cm^2/sec, were used.
Figure 13 shows time of arrival at the bottom sediments for the
Middlesex soil assuming vertical dispersions of 0, 50, and 100
cm^2/sec. The model predicts that at least 95 per cent of the soil
mass would arrive at the sediment surface in less than five days.
Figure 13 indicates that variations in vertical dispersion over the
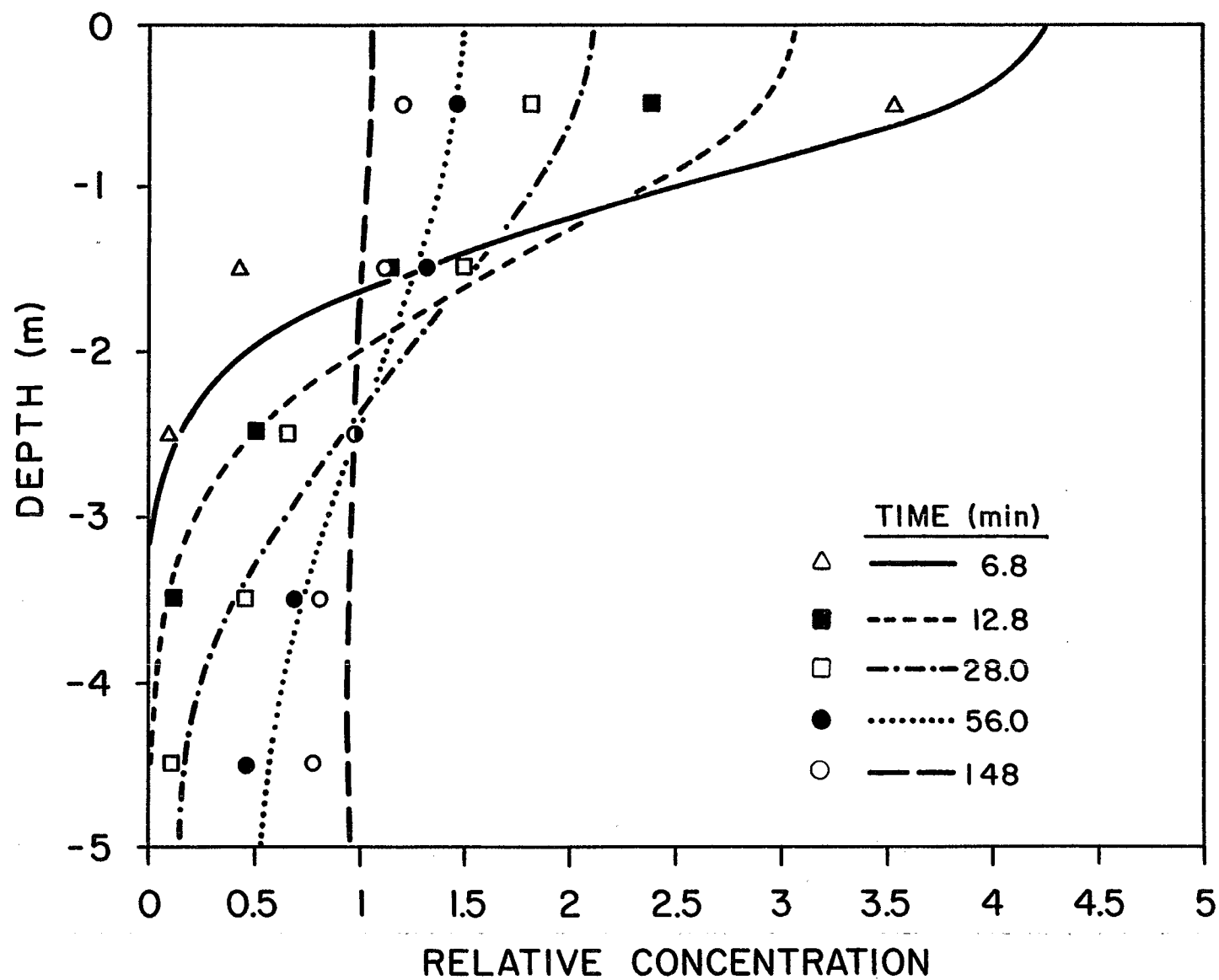range characteristic of deep-ocean sites has negligible effect on the

Figure 12.   Dye experimental results with 11 cm^2/sec dispersion in MERL mesocosm.
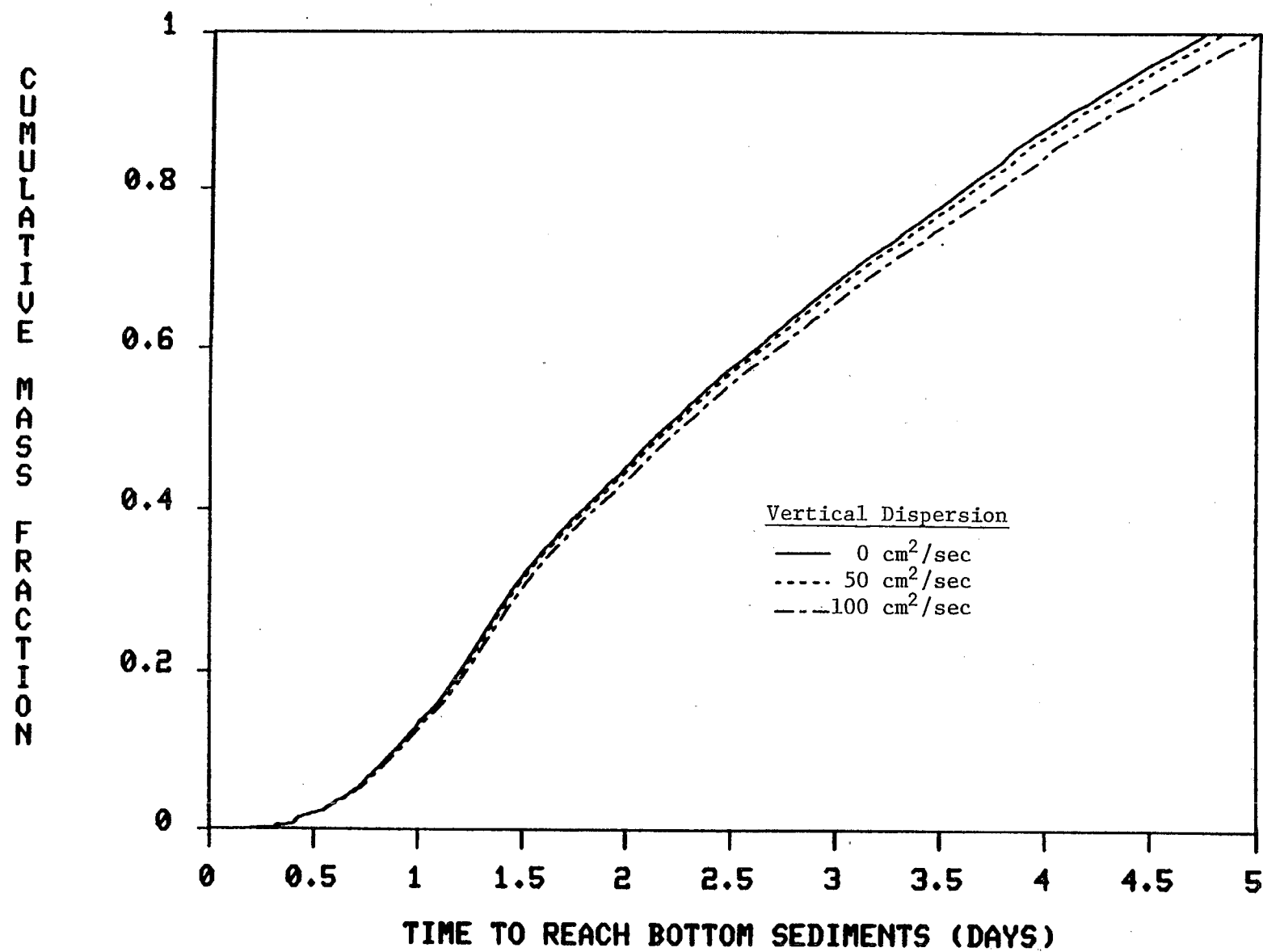
Figure 13. Time of arrival at the bottom of 4000 meter water column for Middlesex soil.

time of arrival for the Middlesex soil.

Information on the horizontal current structure off the northeast coast of the United States (Ingham et al., 1977) was used to calculate the horizontal distance particles would travel before they reach the bottom. The downstream bottom impact distance from the disposal site is shown in Figure 14 for assumed horizontal current velocities of 2.5, 5.0, 7.5 and 10.0 cm/sec. This figure indicates that the distance these particles would travel, for the assumed site condition, ranges from 0.5 to 40.0 km. O'Connor et al. (1985) reported a vertically-weighted mean velocity based on the deep-ocean current structure off the northeast coast of the United States. They determined a mean velocity of approximately 2.0 cm/sec. With this velocity, the impact distance along the direction of mean flow for 95 per cent of the mass would be aproximately 6 km. For practical purposes, the disposed soil would deposit within the confines of a typical disposal site based on a horizontal current of 2.0 cm/sec.

Our projections for a deep-ocean disposal site were based upon experimental data for the Middlesex soil that had been excavated, sieved, and homogenized. If an actual disposal operation were to commence, the physical characteristics of the soil disposed would be expected to be different than that of the homogenized soil we used. However, our results should provide upper-bound estimates on the time of arrival at the bottom sediments and on the bottom impact distance along the direction of mean flow.
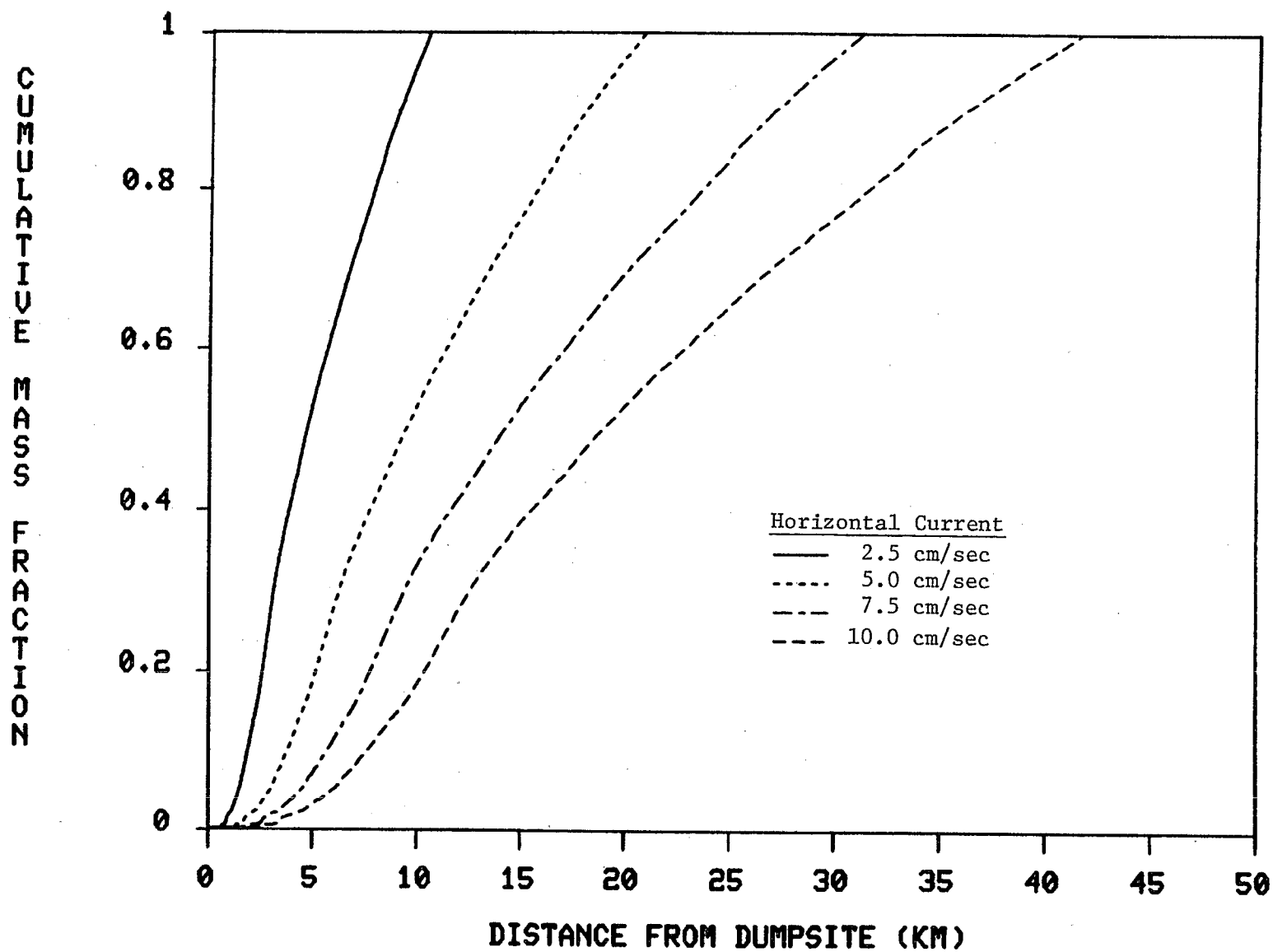
Figure 14. Bottom impact distance along mean flow direction for Middlesex soil disposed in 4000 meters of water.

41

SECTION 5

CONCLUSIONS

A combined experimental and modeling approach was conducted within the framework of the hazard assessment methodology developed at ERLN. Experimentation was conducted to characterize Middlesex soil in terms of particle size distribution, specific gravity, radioactivity, and soluble phase equilibria. In addition, dynamic settling velocity distributions were measured. The data derived from the experimental work were synthesized using a modeling approach that emphasized the vertical convective-diffusive transport of a polydispersed suspension of particles. Ecosystem level studies with Middlesex soil in mesocosms are presented in Hunt (1986). The following conclusions may be drawn from our study:

1. The Middlesex soil in this study had 75 per cent of the mass on particles between 63 and 2000 microns, had a median size of 350 microns, and a bulk specific gravity of 2.31.

2. A measure of gross radioactivity found activity associated with particles sizes from less than 63 to greater than 2000 microns, with a median activity at 125 microns.

3. The specific element or isotope activity distributions showed peaks in activity between 250 and 600 microns. The particle size for median activity distribution of individual isotopes was not coincident with either the size or gross activity distributions.

4. The fraction of total activity which might solubilize upon initial discharge into marine waters was at most 20-24 per cent for the isotopes Ra-226, U-234, U-235, and U-238, and less than 5 per cent for Pb-210, Po-210, and the other isotopes.

5. The velocity distributions were initially dynamic, but tended to converge with increasing depth in a one meter settling column. This indicated that the soil suspension was shifting to a more stable state, and that the velocity distribution was approaching an equilibrium.

6. The measured soil settling velocity ranged up to 8.2 cm/sec, with a median of 2.1 cm/sec.

7. Gravitational settling would be the dominant vertical transport mechanism from Middlesex soil at a deep-ocean disposal site, with vertical dispersion having less than a 5 per cent effect.

8. The Middlesex soil would impact the bottom sediment in 4000 meters of water at distances from 0.5 to 40 km along the direction of mean flow, for horizontal velocities in the

range of 2.5 to 10 cm/sec.

9. Ninety-five per cent of the Middlesex soil disposed in 4000 m of water would arrive at the bottom in less than five days. The particles with the largest settling velocities may reach the bottom in approximately twelve hours.

REFERENCES

Carver, R.E. (ed.) 1971. <u>Procedures in sedimentary petrology</u>. John Wiley and Sons, New York.

Csanady, G.T. 1973. <u>Turbulent diffusion in the environment</u>. D. Reidel Publishing Co., Boston.

Hunt, C.D. 1986. Fate and bioaccumulation of soil-associated low-level natural radioactivity discharged into a marine ecosystem. Report in preparation.

Kupferman, S.L., D.R. Anderson, L.H. Brush, L.S. Gomez, and L.E. Shephard. 1984. FODOCS Annual Report March 1 – September 30, 1981. Rept. SAND82-0292, Sandia National Laboratories, Albuquerque, New Mexico. 68 pp.

Ingham, M.C., J.J. Bisagni, and D. Mizenko. 1977. The general physical oceanography of Deepwater Dumpsite 106. In: Baseline Report of Environmental Conditions at Deepwater Dumpsite 106, Vol. 1. NOAA Dumpsite Evaluation Rept. 77-1, U.S. Dept. of Comm. Pub., pp. 29-54.

Lick, W. 1982. Entrainment, deposition, and transport of fine-grain sediments in Lakes. <u>Hydrobiologia</u>, 91:31-40.

Nixon, S.W., D. Alonso, M.E.Q. Pilson, and B.A. Buckley. 1980. Turbulent mixing in aquatic microcosms. In: Microcosms in Ecological Research, G.P. Gisey (ed.). DOE Symposium Series, Augusta, Georgia, Nov. 8-10, 1978. CONF-781101, NTIS, pp. 818-849.

O'Connor, T.P., H.A. Walker, J.F. Paul, and V.J. Bierman, Jr. 1985. A strategy for monitoring of contaminant distributions resulting from proposed sewage sludge disposal at the 106-Mile Ocean Disposal Site. <u>Marine Environmental Research</u>, 16:127-150.

Prager, J.C., V.J. Bierman, Jr., J.F. Paul, and J.S. Bonner. 1984. Hazard assessment of low level radioactive wastes. A proposed approach to ocean dumping permit request analyses. Technical Report, Environmental Research Laboratory, U.S. Environmental Protection Agency, Narragansett, Rhode Island.

U.S. Congress P. L. 92-532. The Marine Protection, Research and Sanctuaries Act of 1972, 33 U. S. 1401 et. seq.

Weber, W.J., Jr. 1972. <u>Physiochemical processes for water quality control</u>. Wiley-Interscience, New York.
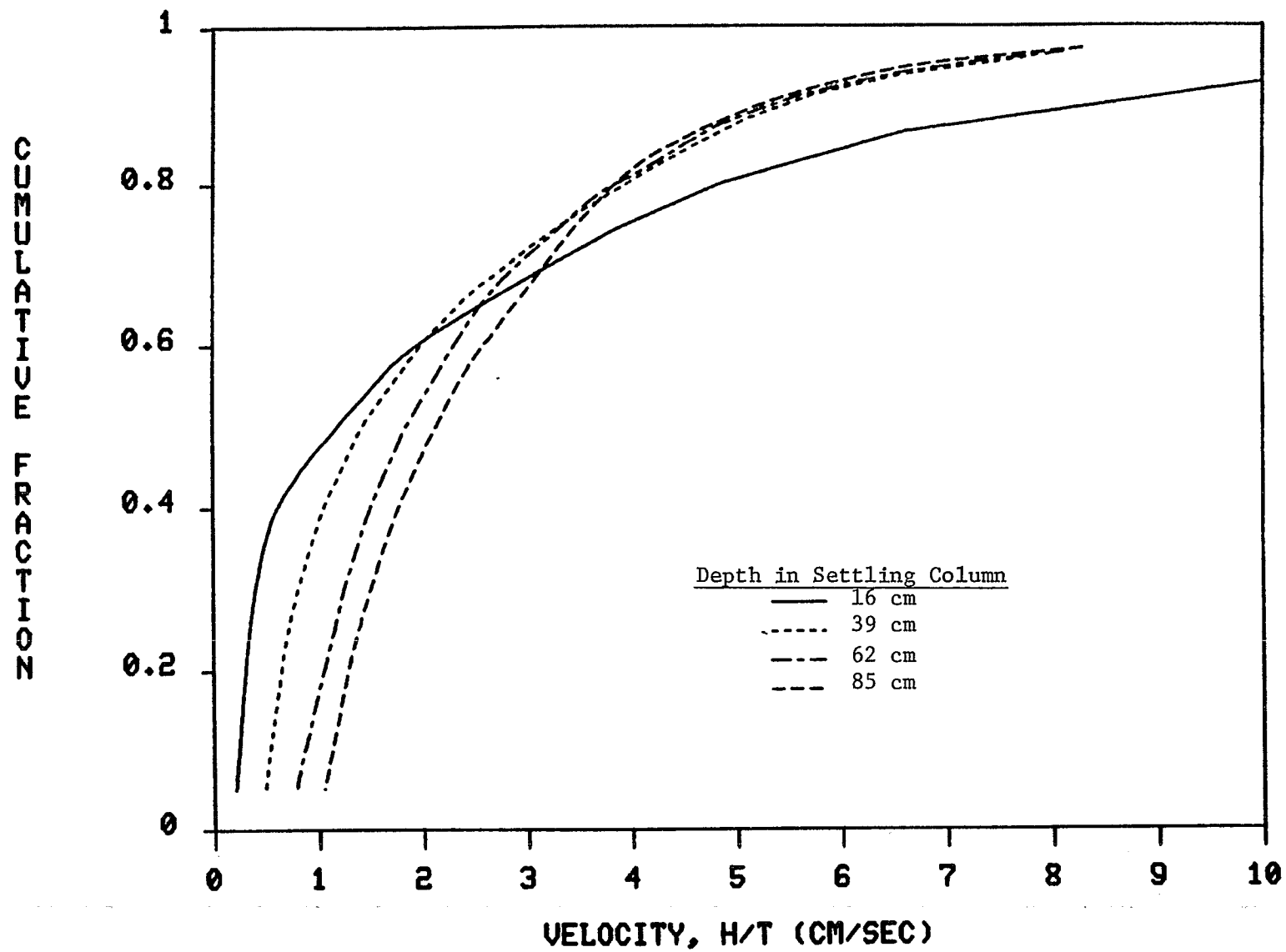
APPENDIX A

BENCH–SCALE SETTLING VELOCITY DATA

Figure A-1. Settling velocity distribution for Middlesex soil determined from laboratory column experiments.
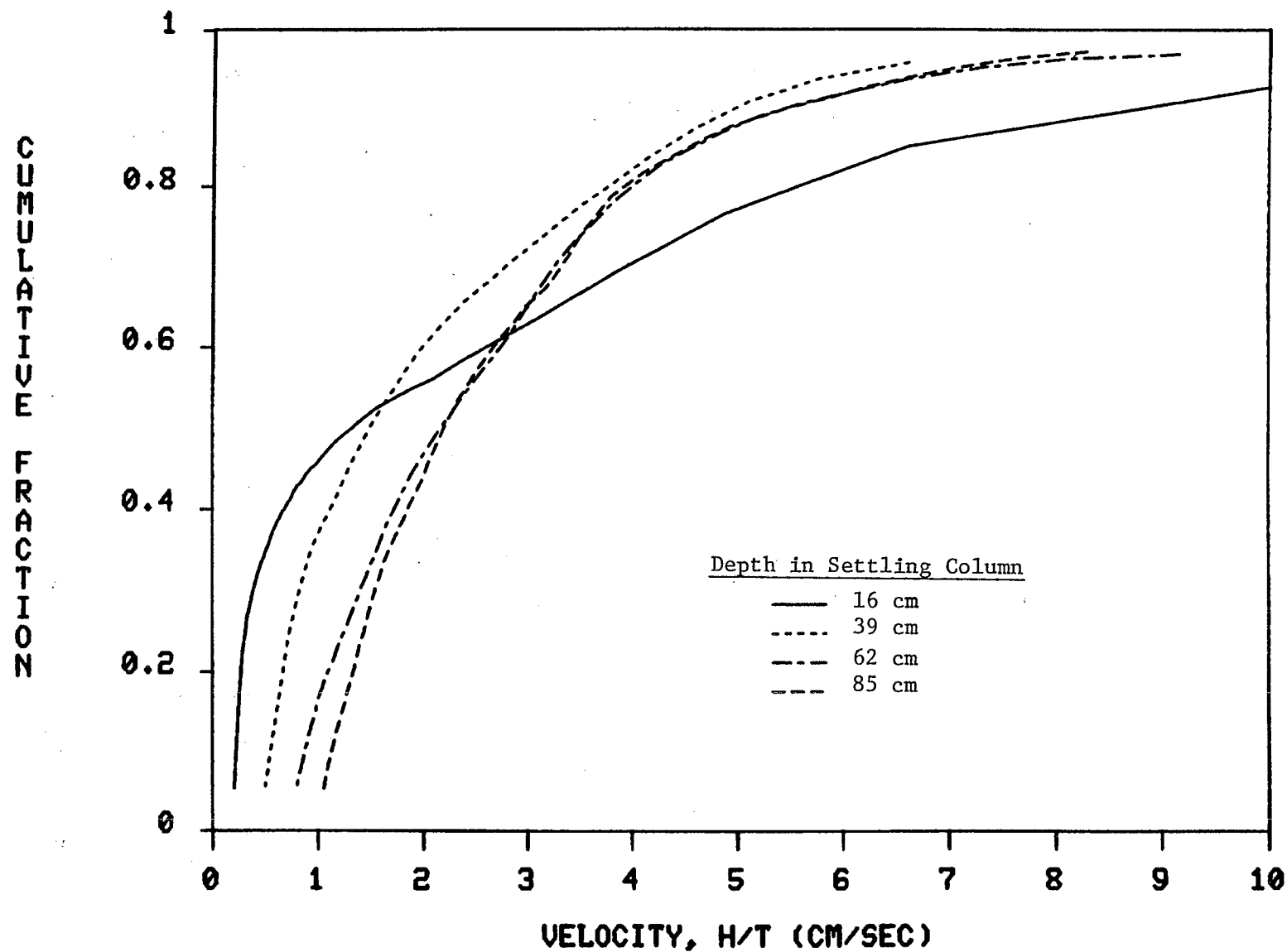
Figure A-2. Settling velocity distribution for Middlesex soil determined from
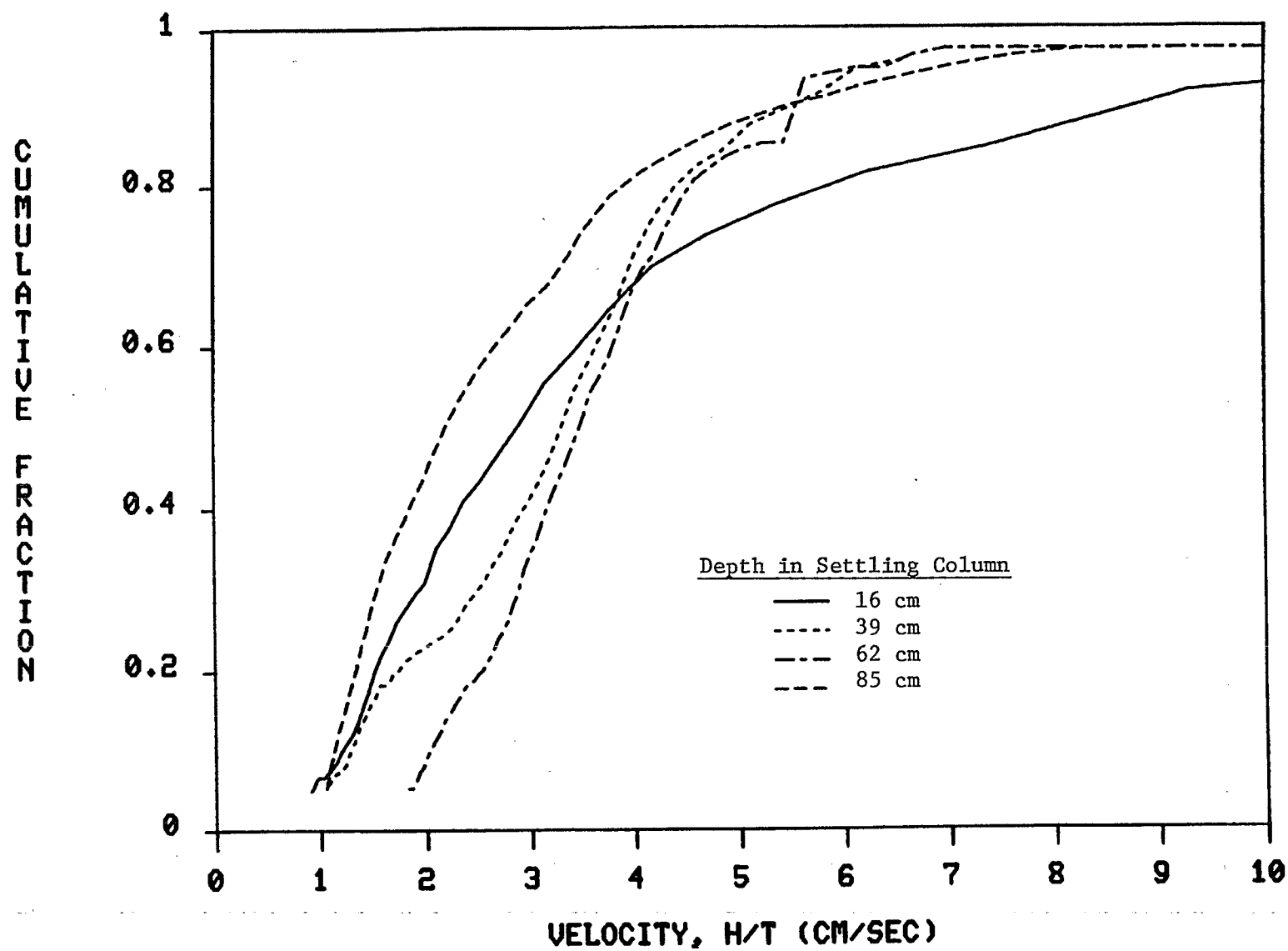laboratory column experiments.

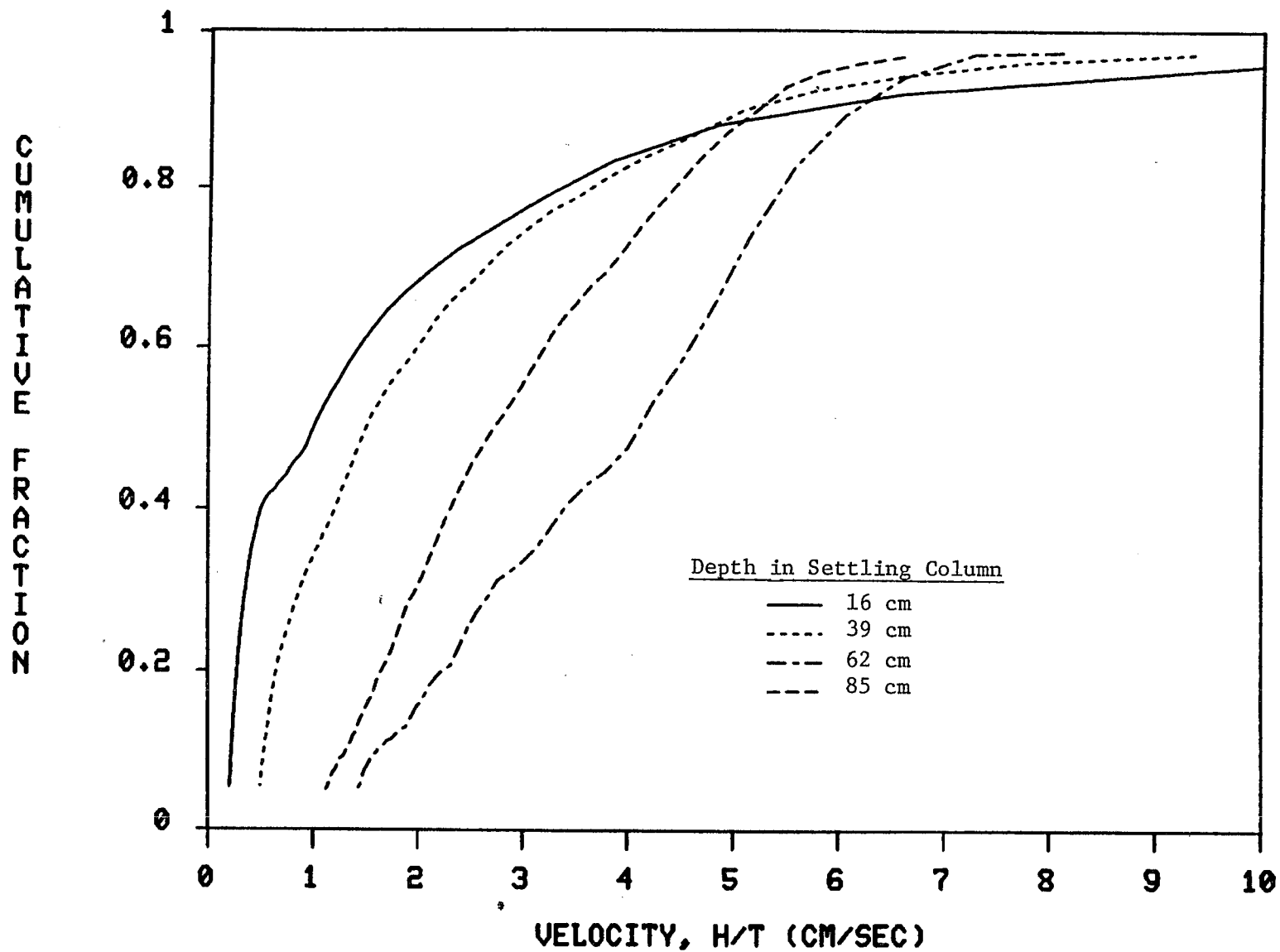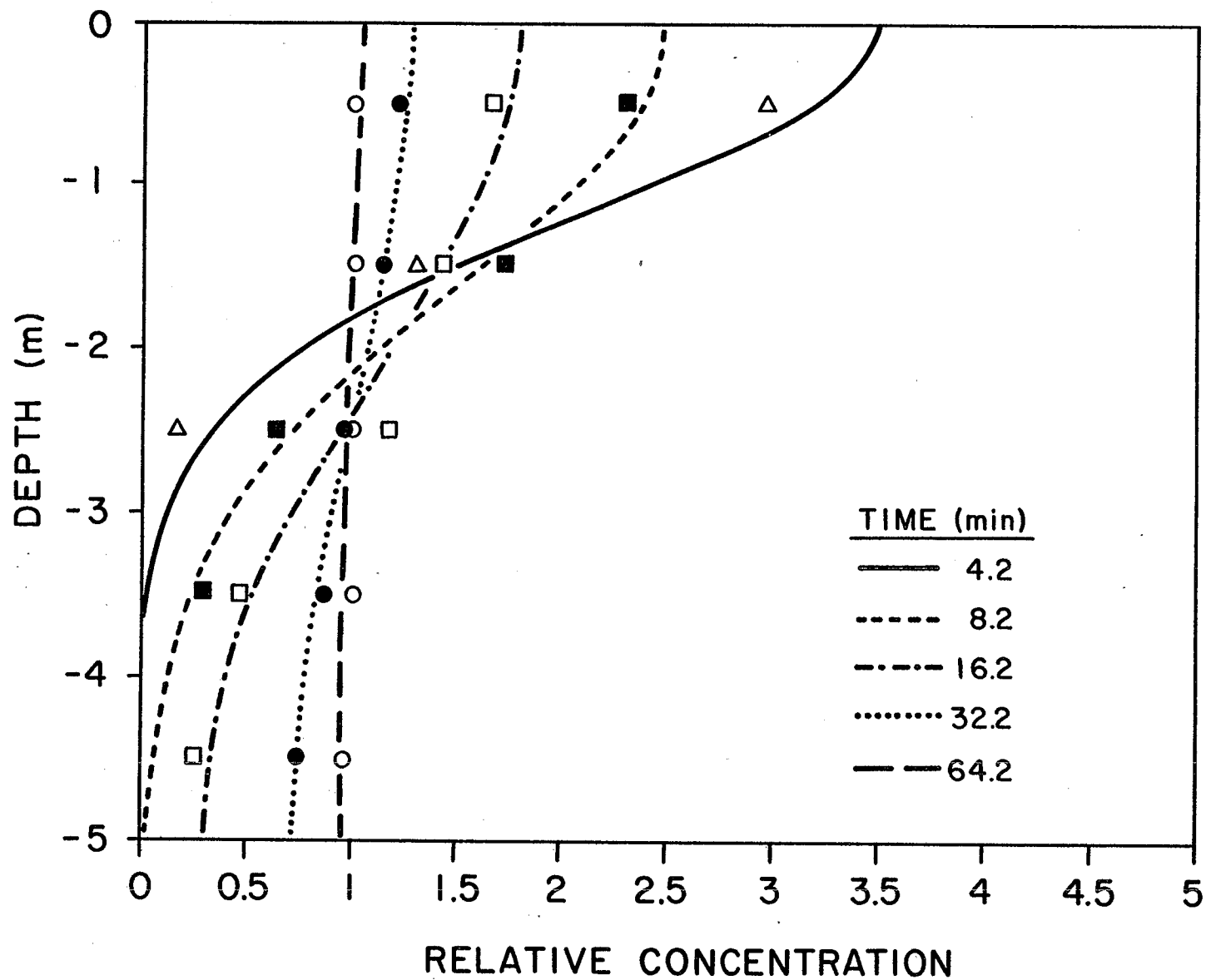Figure A-3. Settling velocity distribution for Middlesex soil determined from laboratory column experiments.

Figure A-4.   Settling velocity distribution for Middlesex soil determined from laboratory column experiments.

APPENDIX B

MESOCOSM–SCALE DATA

Figure B-1. Dye experimental results with 8 cm^2/sec dispersion in MERL mesocosm.
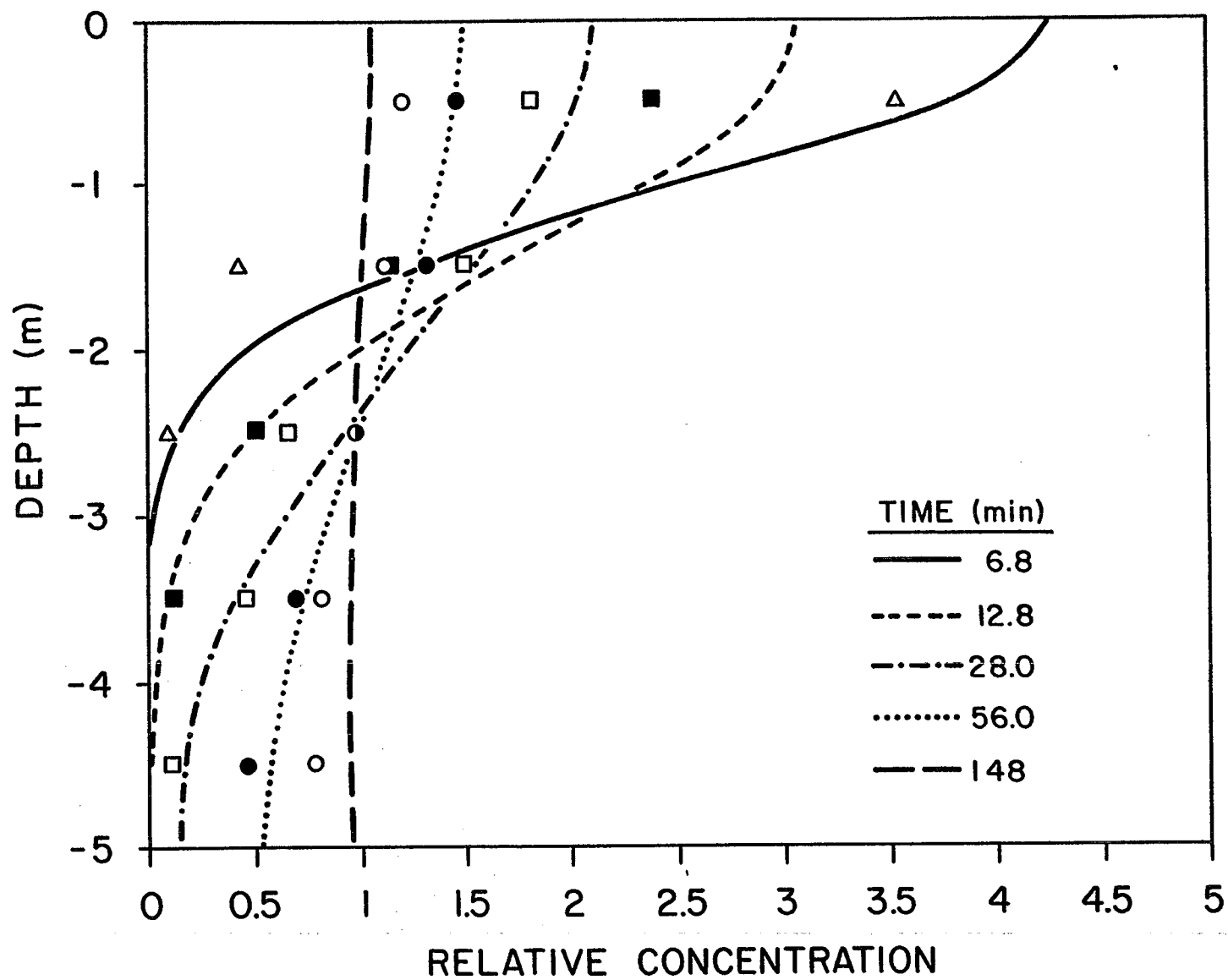
Figure B-2. Dye experimental results with 11 cm^2/sec dispersion in MERL mesocosm.
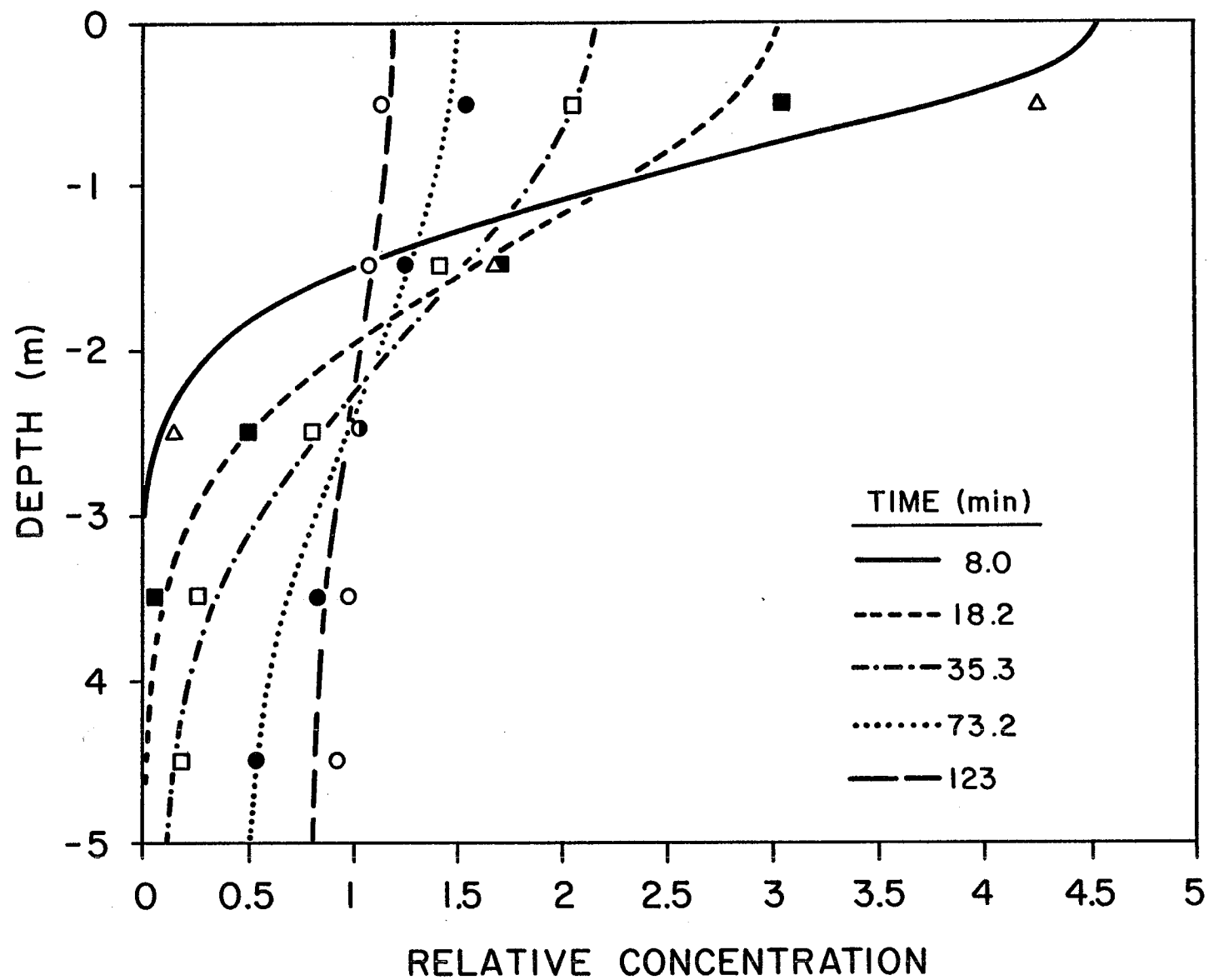
Figure B-3. Dye experimental results with 26 cm^2/sec dispersion in MERL mesocosm.
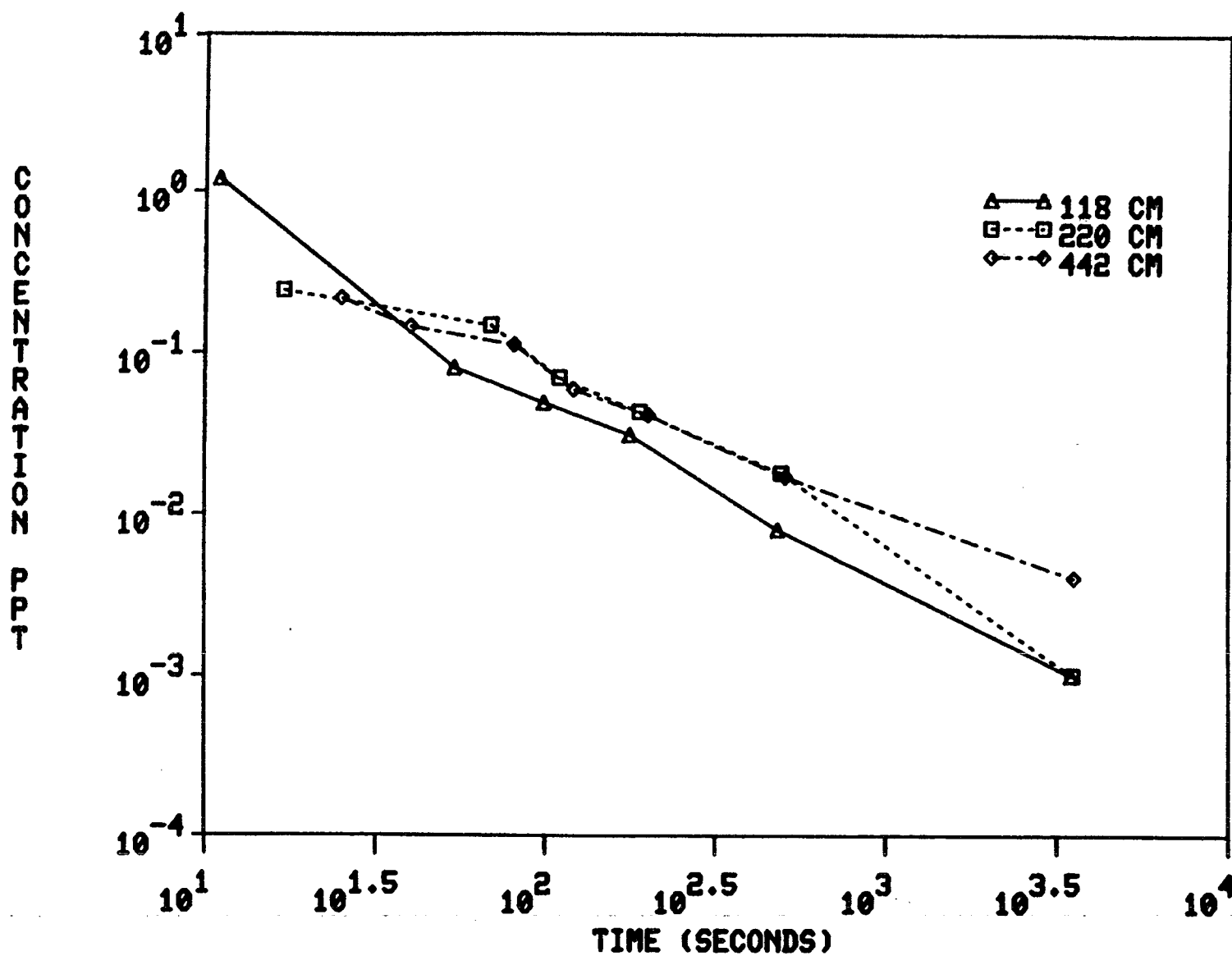
Figure B-4. Mass removal experimental results for particles greater than 63 microns and with 26 cm^2/sec dispersion in MERL mesocosm.
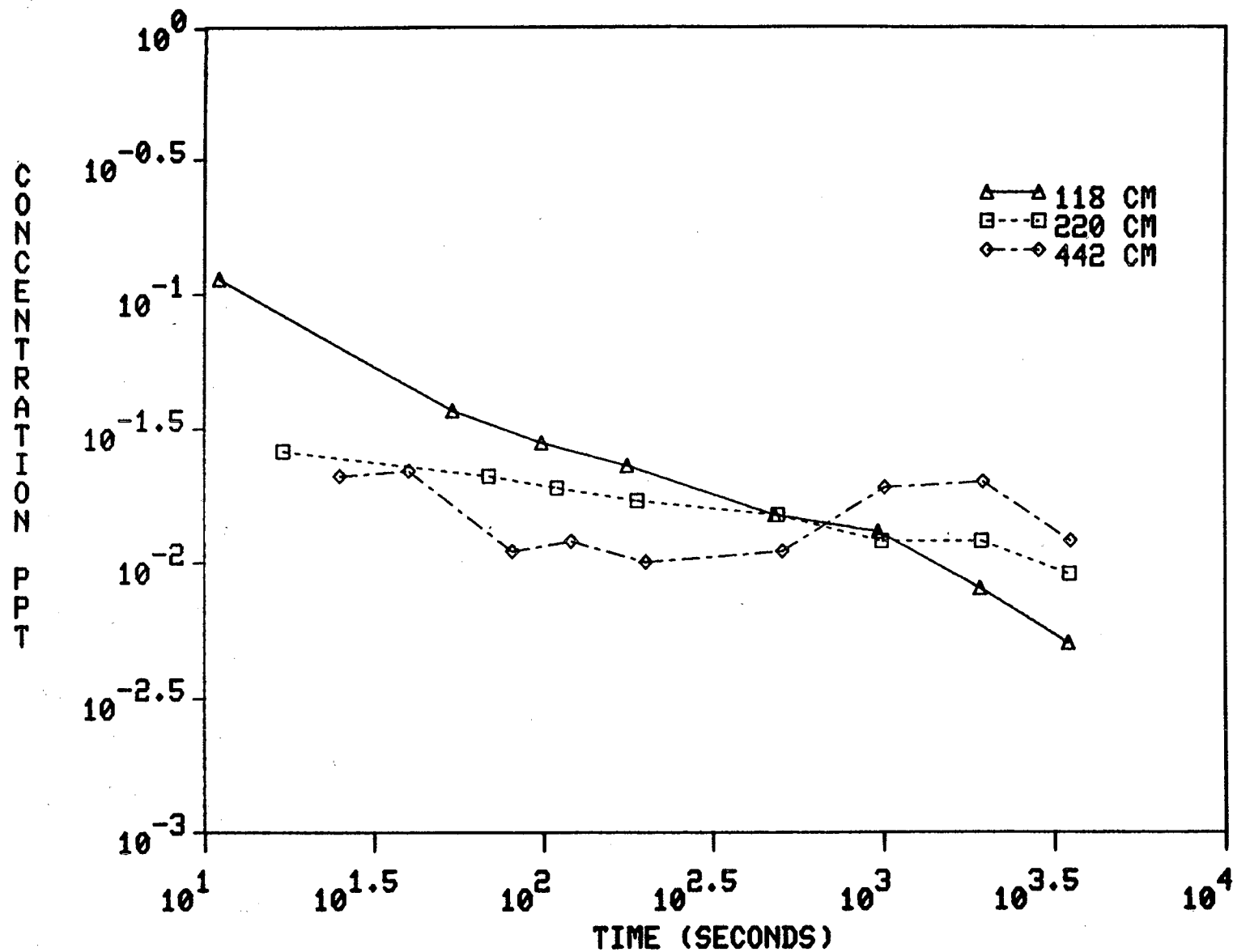
Figure B-5. Mass removal experimental results for particles less than 63 microns and with 26 cm^2/sec dispersion in MERL mesocosm.
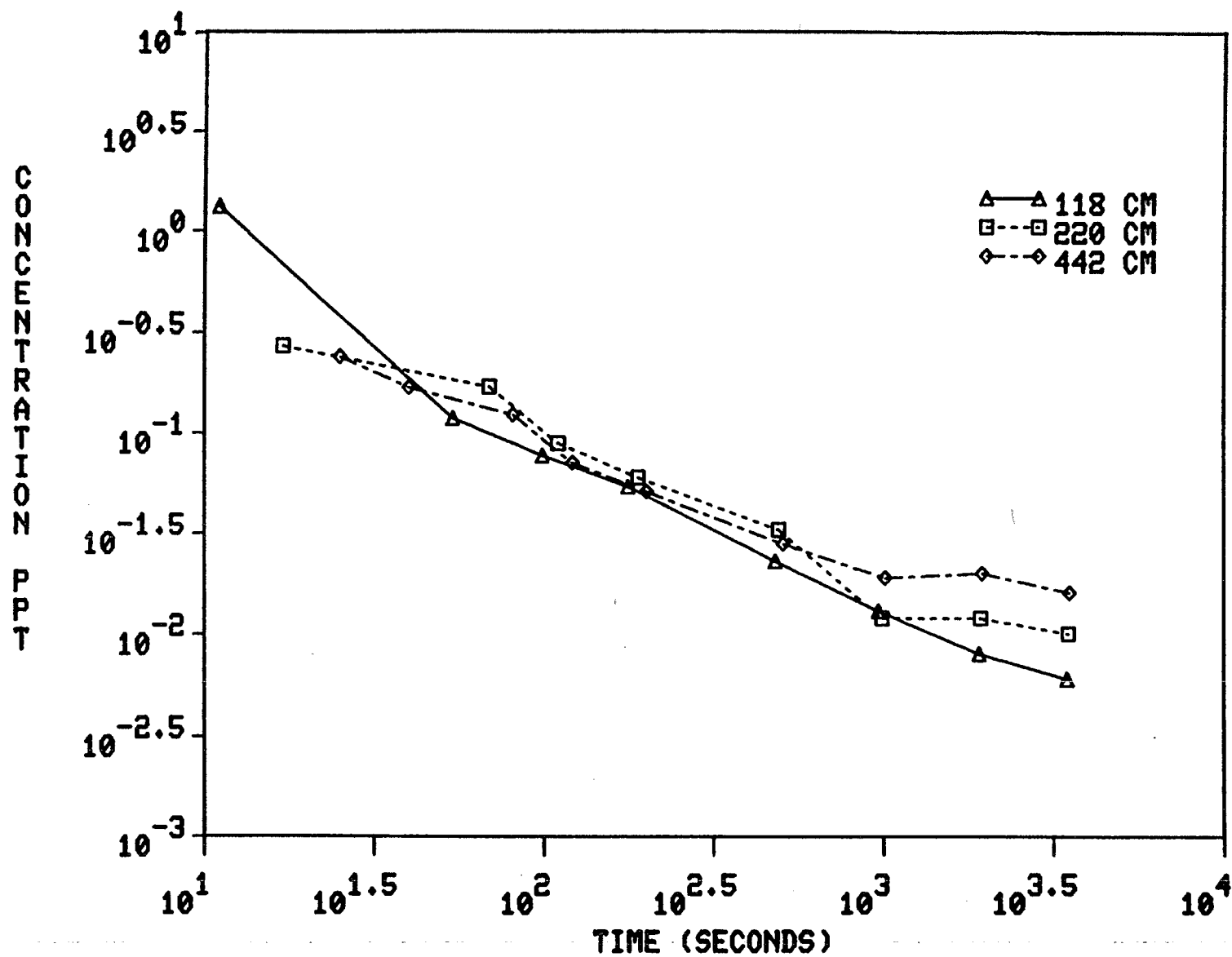
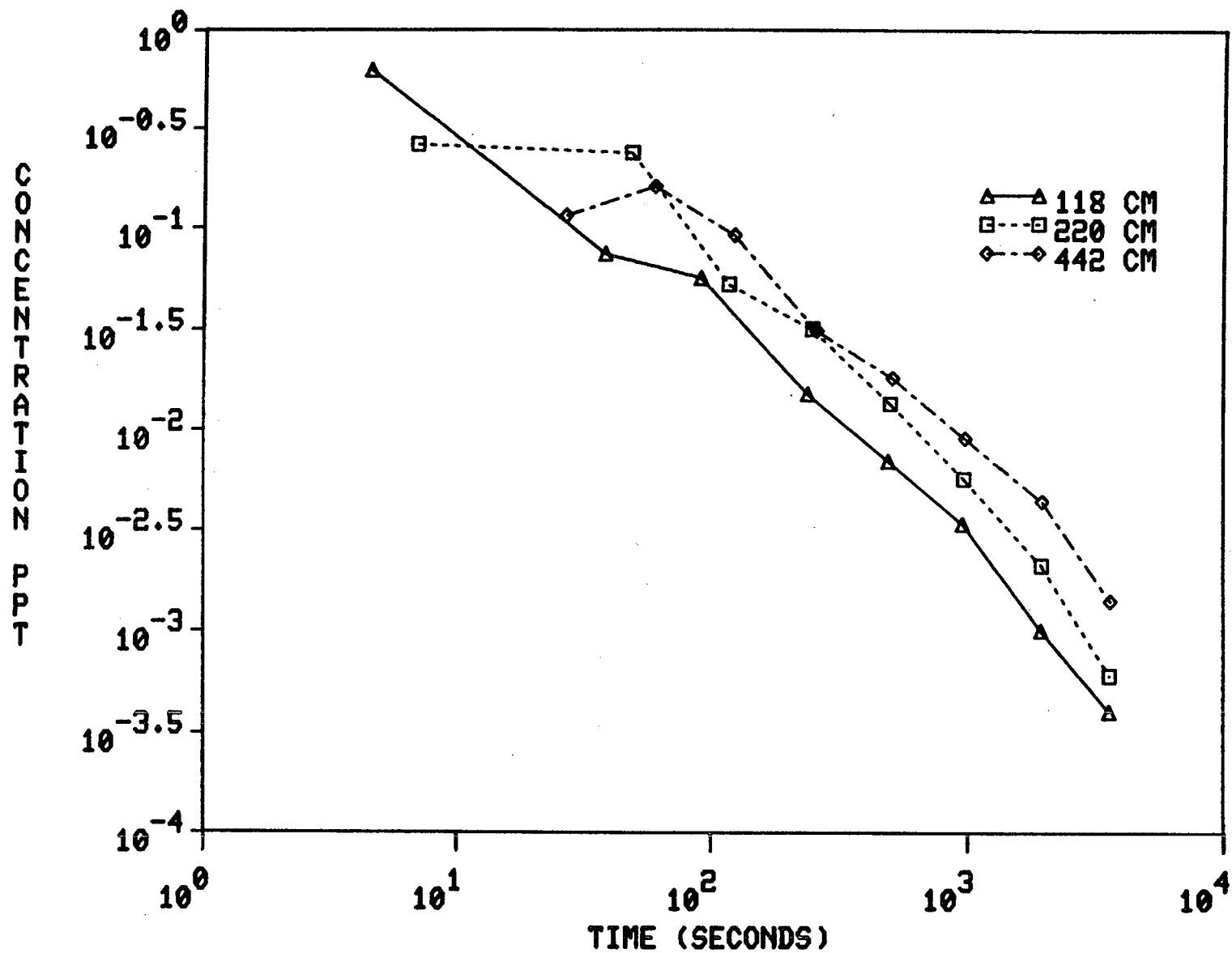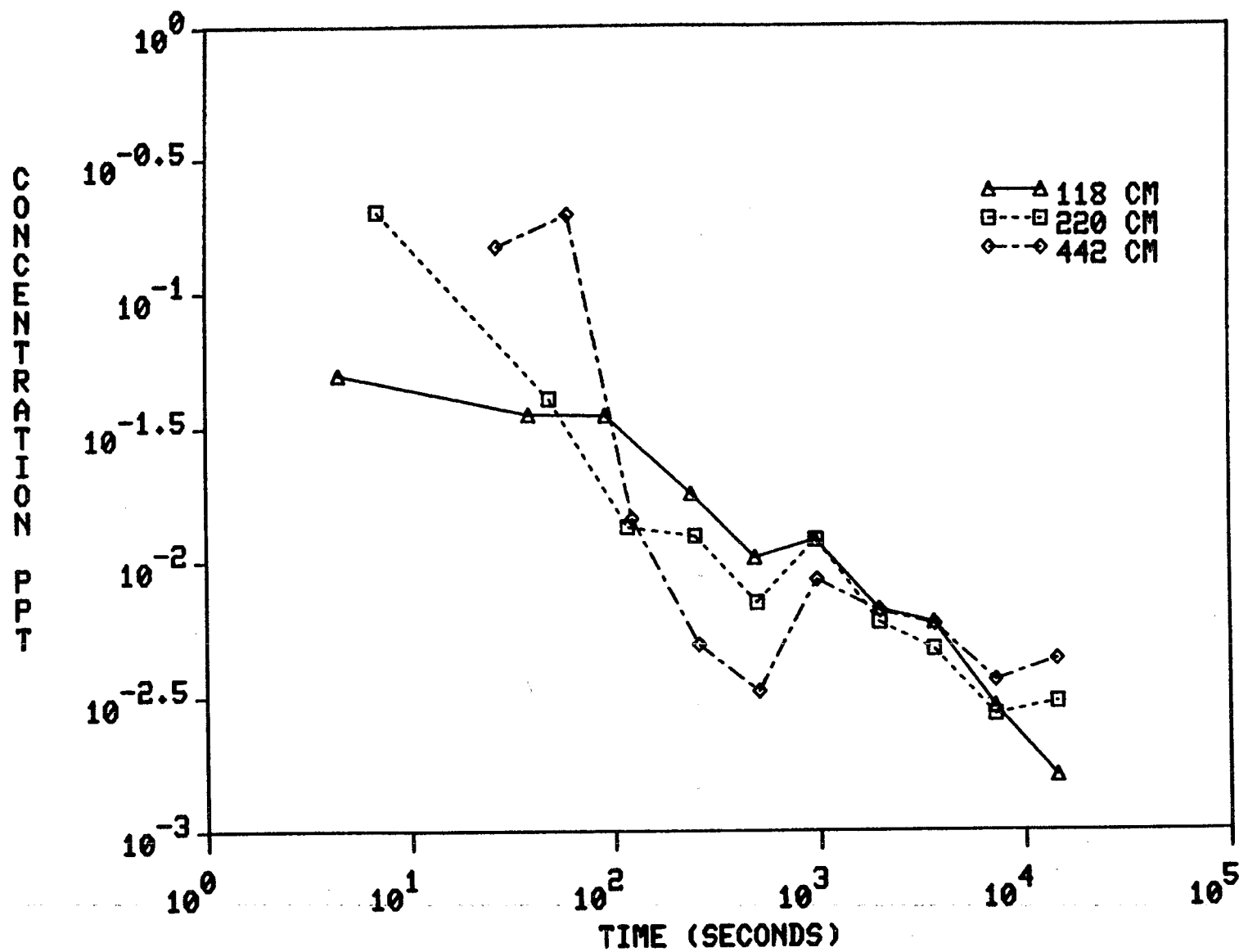Figure B-6. Mass removal experimental results for total mass and with 26 cm^2/sec dispersion in MERL mesocosm.

Figure B-7.   Mass removal experimental results for particles greater than 63 microns and with 11 cm^2/sec dispersion in MERL mesocosm.

Figure B-8.   Mass removal experimental results for particles less than 63 microns and with 11 cm^2/sec dispersion in MERL mesocosm.
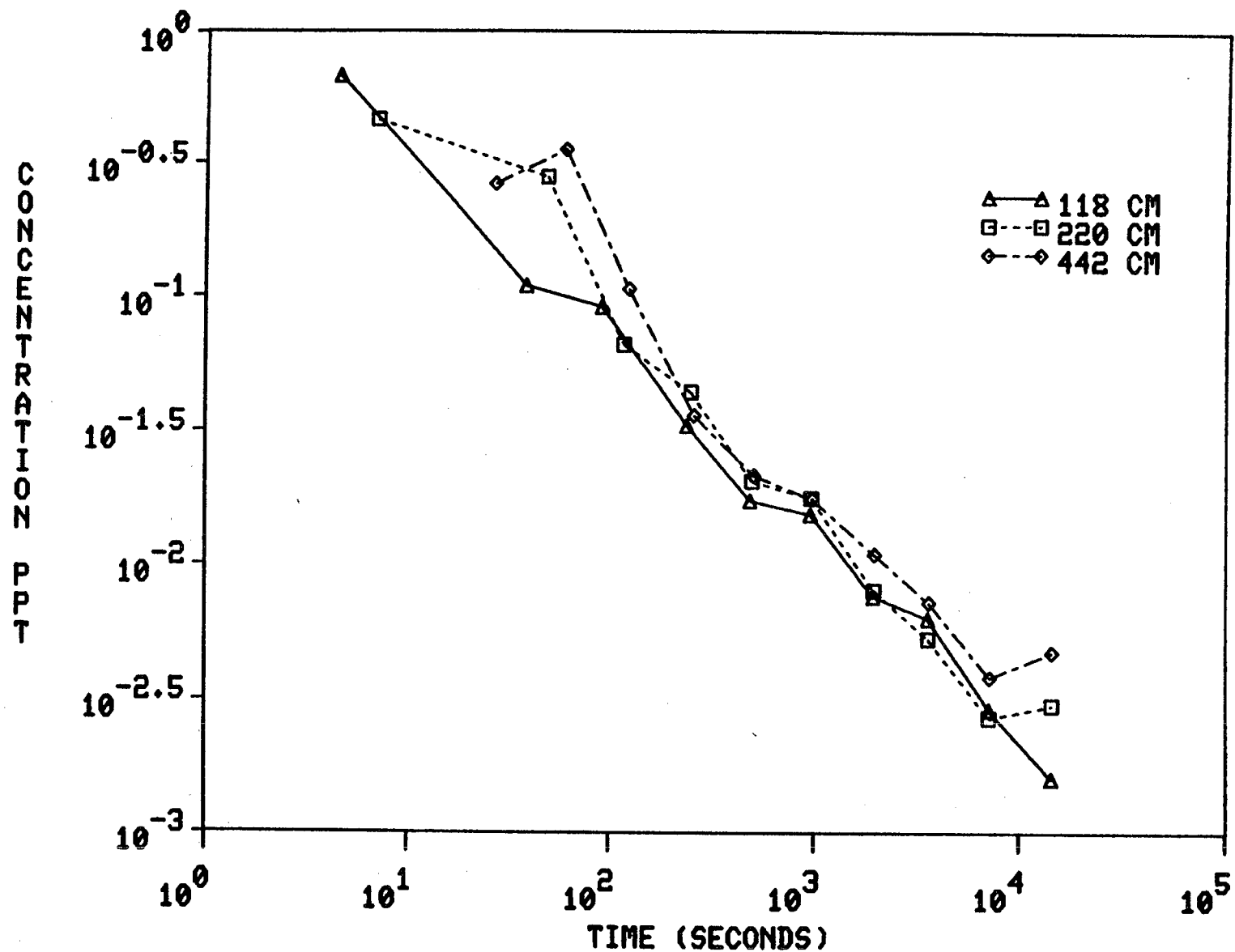
Figure B-9. Mass removal experimental results for total mass and with 11 cm^2/sec dispersion in MERL mesocosm.
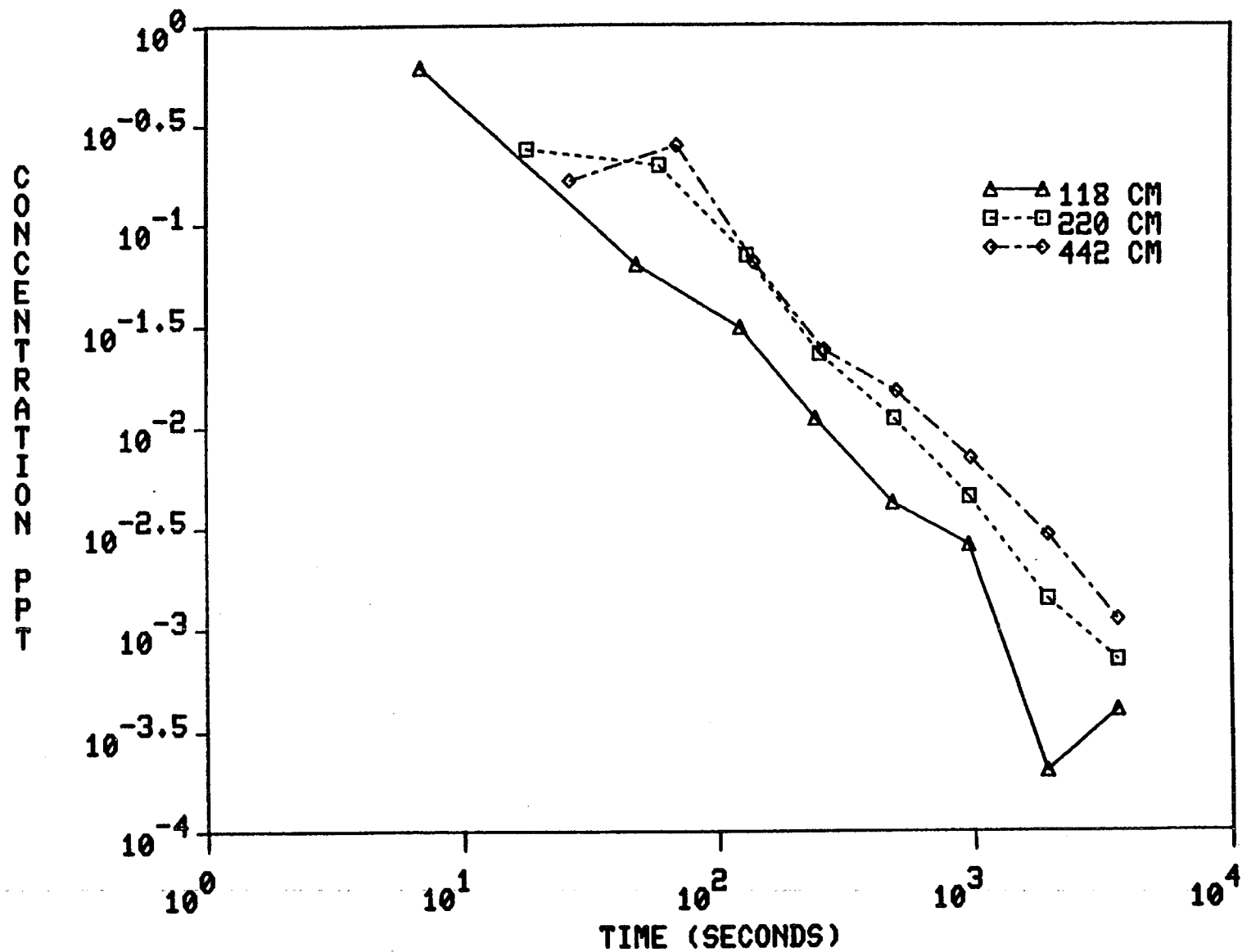
Figure B-10. Mass removal experimental results for particles greater than 63 microns and with 8 cm^2/sec dispersion in MERL mesocosm.